



8-2004

Development of a Reagentless Amperometric Ethanol Biosensor Based on Yeast Alcohol Dehydrogenase and its Coenzyme, NAD⁺, Coimmobilized on a Carbon Nanotubes- modified Electrode

Justin Matthew Holland
University of Tennessee, Knoxville

Follow this and additional works at: https://trace.tennessee.edu/utk_gradthes

 Part of the [Chemical Engineering Commons](#)

Recommended Citation

Holland, Justin Matthew, "Development of a Reagentless Amperometric Ethanol Biosensor Based on Yeast Alcohol Dehydrogenase and its Coenzyme, NAD⁺, Coimmobilized on a Carbon Nanotubes- modified Electrode. " Master's Thesis, University of Tennessee, 2004.
https://trace.tennessee.edu/utk_gradthes/4809

This Thesis is brought to you for free and open access by the Graduate School at TRACE: Tennessee Research and Creative Exchange. It has been accepted for inclusion in Masters Theses by an authorized administrator of TRACE: Tennessee Research and Creative Exchange. For more information, please contact trace@utk.edu.

To the Graduate Council:

I am submitting herewith a thesis written by Justin Matthew Holland entitled "Development of a Reagentless Amperometric Ethanol Biosensor Based on Yeast Alcohol Dehydrogenase and its Coenzyme, NAD⁺, Coimmobilized on a Carbon Nanotubes- modified Electrode." I have examined the final electronic copy of this thesis for form and content and recommend that it be accepted in partial fulfillment of the requirements for the degree of Master of Science, with a major in Chemical Engineering.

Paul Frymier, Major Professor

We have read this thesis and recommend its acceptance:

Brian Davison, Cynthia Peterson

Accepted for the Council:

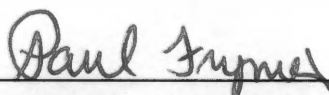
Carolyn R. Hodges

Vice Provost and Dean of the Graduate School

(Original signatures are on file with official student records.)

To the Graduate Council:

We are submitting herewith a thesis written by Justin Matthew Holland entitled "Development of a Reagentless Amperometric Ethanol Biosensor Based on Yeast Alcohol Dehydrogenase and its Coenzyme, NAD⁺, Coimmobilized on a Carbon Nanotubes- modified Electrode". We have examined the final paper copy of this thesis for form and content and recommend that it be accepted in partial fulfillment of the requirements for the degree of Master of Science, with a major in Chemical Engineering.

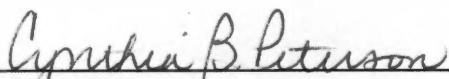


Paul Frymier, Major Professor

We have read this thesis and recommend its acceptance:



Brian Davison



Cynthia Peterson

Accepted for the Council:



Vice Chancellor and Dean of Graduate Studies

**DEVELOPMENT OF A REAGENTLESS AMPEROMETRIC ETHANOL
BIOSENSOR BASED ON YEAST ALCOHOL DEHYDROGENASE AND ITS
COENZYME, NAD⁺, COIMMOBILIZED ON A CARBON NANOTUBES-
MODIFIED ELECTRODE**

**A Thesis
Presented for the
Master of Science
Degree
The University of Tennessee, Knoxville**

**Justin Matthew Holland
August 2004**

Thesis
2004
H65

Copyright © 2004 by Justin Matthew Holland

All rights reserved

DEMOCRACY
SOUTH*WORTH
COLLECTION

DEDICATION

I dedicate this thesis to my lovely fiancée, whose advice and support provide a constant source of encouragement, and my unborn son, who will surely be the light of my life.

ACKNOWLEDGEMENTS

I would like to thank my thesis advisor, Dr. Paul Frymier, for his insight and guidance in my research and professional development. In addition, I am indebted to my thesis committee members, Dr. Brian Davison and Dr. Cynthia Peterson for their invaluable contributions to my thesis. The contributions of Dr. David Nivens and Dr. Jim Chambers in knowledge and equipment are also greatly appreciated. I am grateful for the funding provided by Eastman Chemical and the Center for Environmental Biotechnology at the University of Tennessee. Finally, I would like to thank my family and friends who have been a constant source of support.

ABSTRACT

A reagentless amperometric ethanol biosensor was fabricated by modifying a glassy carbon (GC) electrode with a thin film of multi-walled carbon nanotubes (MWNTs) and depositing yeast alcohol dehydrogenase (YADH) and its coenzyme, nicotinamide adenine dinucleotide (NAD^+), on the surface of the modified electrode. The enzyme was immobilized on the modified electrode using two techniques: adsorption and covalent attachment. Biosensors based on graphite and carbon nanofibers (CNFs) were also fabricated in a similar manner except that the enzyme was only adsorbed to the electrode surface.

The performance of the biosensors was assessed using a number of analytical techniques. Cyclic voltammetry was employed to determine the peak potential of NADH oxidation for each biosensor. Amperometric measurements were then conducted at or near the peak potential and the current response of each biosensor to successive ethanol additions was evaluated. The two MWNT-based biosensors with adsorbed and covalently attached YADH were subjected to more detailed analysis including evaluation of stability, reusability and linear concentration range.

The MWNT-based biosensor was found to exhibit a much higher current response to ethanol than the graphite- and CNF-based biosensors at a working potential of +0.3 V (vs. Ag/AgCl). In addition, it displayed a relatively quick and stable response to individual ethanol additions. Both the adsorbed and covalently attached MWNT-biosensors had large linear concentration ranges, excellent stability and similar reusabilities.

TABLE OF CONTENTS

CHAPTER	PAGE
1. INTRODUCTION.....	1
2. BACKGROUND	4
2.1 Fundamentals of Enzyme-based Amperometric Biosensors.....	7
2.2 Designing Enzyme-based Amperometric Biosensors.....	12
2.2.1 Amperometric Detection of Redox-active Species	13
2.2.2 Enzyme Stabilization Techniques	16
2.2.3 Working Electrode Materials	18
2.3 Evaluation of Enzyme-based Amperometric Biosensors.....	21
2.4 Design Considerations for a YADH-based Biosensor	26
2.4.1 Amperometric Detection of NADH.....	28
2.4.2 Carbon Nanomaterials as Working Electrode Materials.....	29
2.4.3 YADH Immobilization on Carbon Nanomaterials	32
2.4.4 Design Proposal for a YADH-based Biosensor	33
3. MATERIALS AND METHODS.....	35
3.1 Reagents	35
3.2 Apparatus.....	35
3.3 Fabrication of the Ethanol Biosensor.....	36

4. RESULTS AND DISCUSSION	38
4.1 Electrochemical NADH Oxidation at Graphite-, CNF- and MWNT-modified GC Electrodes.....	38
4.2 Electrochemical Ethanol Detection by Graphite-, CNF- and MWNT-based Biosensors	46
4.3 Enzyme Surface Coverage on the MWNT-based Biosensor	50
4.4 Enzyme Kinetics of the MWNT-based Biosensor	51
4.5 Storage Stability of the MWNT-based Biosensor.....	61
4.6 Reusability of the MWNT-based Biosensor	61
5. CONCLUSION.....	64
BIBLIOGRAPHY	66
VITA.....	71

LIST OF TABLES

TABLE	PAGE
2.1 Examples of previously developed enzyme-based amperometric ethanol biosensors	27
4.1 Kinetic model parameters for MWNT-based biosensors and a MWNT-modified electrode	58

LIST OF FIGURES

FIGURE	PAGE
2.1 The different kinds of biological elements and transducers used in biosensors and the general principles of how they function	5
2.2 Schematic representation of a potentiostat and three-electrode cell	8
2.3 A hypothetical enzyme-based amperometric biosensor	10
2.4 Examples of indirect analyte detection techniques	15
2.5 Common covalent immobilization techniques for enzymes	19
2.6 Hypothetical cyclic voltammograms for two materials	23
2.7 Apparent enzyme kinetics of a biosensor for different rate-determining steps	25
2.8 Scanning electron micrograph of CNFs grown on a silicon support	31
2.9 Covalent attachment of an enzyme to CNTs/CNFs via EDAC-activated amidation	34
4.1 Cyclic voltammogram for an unmodified GC electrode in 1 mM NADH ...	39
4.2 Cyclic voltammogram for a graphite-modified GC electrode in 1 mM NADH	40
4.3 Cyclic voltammogram for a CNF-modified GC electrode in 1 mM NADH	42
4.4 Cyclic voltammogram for a MWNT-modified GC electrode in 1 mM NADH	43

4.5	Cyclic voltammograms for unmodified, graphite-, CNF- and MWNT-modified GC electrodes in 1 mM NADH	44
4.6	Amperometric detection of NADH at graphite-, CNF- and MWNT-modified GC electrodes	45
4.7	Amperometric detection of ethanol by graphite-, CNF- and MWNT-based biosensors.....	48
4.8	Individual responses of different biosensors to ethanol additions	49
4.9	Amperometric detection of ethanol by two different MWNT-based biosensors.....	53
4.10	Current as a function of ethanol concentration for two different MWNT-based biosensors.....	54
4.11	Amperometric detection of ethanol by the MWNT-modified electrode with YADH and NAD ⁺ in free solution.....	55
4.12	Current as a function of ethanol concentration for the MWNT-modified electrode with YADH and NAD ⁺ in free solution	56
4.13	Reusability of two different MWNT-based biosensors	62

CHAPTER 1 INTRODUCTION

The field of sensor technology has experienced significant growth in recent years, driven by the chemical analysis needs of industry and government. Sensors are frequently used for quantitative detection of analytes in environmental monitoring and process monitoring in the agriculture, food and drug industries. The primary advantage of sensors over traditional analytical techniques is that they can be employed *in vivo* to monitor analyte concentration continuously and in real-time, whereas the latter are typically limited to intermittent analysis [1]. The *in vivo* application of sensors requires that they be able to discriminate between the analyte and any other components that may be present. In other words, a sensor must possess adequate specificity for its analyte, and this has been one of the major challenges encountered in sensor development.

Although many different kinds of sensors have been developed, they all function in the same fundamental manner by transducing a physical or chemical parameter into an electrical or optical signal. Some examples of transducers that have been used in sensors include electrochemical, piezoelectric, magnetic and thermometric [2]. Electrochemical transducers, in particular, have been used extensively in developing sensors for chemical analysis due to the relative simplicity and low cost of their implementation. While potentiometric electrochemical sensors have been successfully employed in the detection of hydrogen ions, various metal

ions, and some non-metal ions, they are quite ineffective at detecting many organic compounds. Amperometric sensors are more amenable to detection of organic compounds since their potential can be controlled. However, there are many compounds which are not redox-active and are difficult to detect using traditional electrochemical biosensors. This serious limitation has prompted researchers to investigate the combination of highly specific enzymes with electrochemical sensors. These so-called “biosensors” have significantly expanded the number of analytes detectable by electrochemical means, as reflected by the well over 1000 publications on the subject since 1995 [1].

Most electrochemical biosensors function by converting the desired analyte into a more readily detectable species. That is, an enzyme which will catalyze a reaction involving the analyte is chosen such that, upon reaction, an ionic species or other electrochemically active species is produced and can subsequently be detected by the biosensor. For some types of enzymes, such as the oxidoreductases, analyte detection can be accomplished by detecting the oxidized or reduced form of the coenzyme produced by the enzyme-catalyzed reaction. It should be stated that the material used for the electrochemical transducer can have a major impact on the sensitivity of the biosensor to the species produced by the enzyme. Indeed, one of the hurdles frequently encountered in biosensor development is finding a suitable material for the transducer [3]. There are some additional disadvantages associated with biosensors. For example, the conditions under which they can operate are limited by the sensitivity of enzymes to pH, temperature and ionic strength. Also,

their use is limited mainly to aqueous solutions and their dynamic ranges can be small [4]. Researchers have made progress in overcoming these barriers for a large number of biosensors, yet there still remain some biosensors that have proven to be problematic in their development and implementation.

The aim of this thesis is to develop an electrochemical ethanol biosensor based upon the enzyme yeast alcohol dehydrogenase (YADH) and its coenzyme, nicotinamide adenine dinucleotide (NAD^+). Since relatively little work has been done on this particular biosensor, it is an excellent choice for further development. In the next chapter, previous research in the development of amperometric biosensors is discussed and rationale are given for the design choices made in the development of the new ethanol biosensor.

CHAPTER 2 BACKGROUND

Biosensors enable highly selective and sensitive detection of analytes by taking advantage of the specificity provided by biological elements such as enzymes, antibodies and organelles. In order to generate an electrical or optical signal, the biological elements are coupled with signal transducers. The large variety of biological elements and transducers available allow one to design a biosensor for a particular analyte by choosing a unique physical or chemical characteristic of the analyte to measure. For example, detection of an analyte on the basis of its weight could be achieved by coupling a high-affinity antibody with a piezoelectric transducer [5]. Figure 2.1 shows many of the combinations of biological elements and transducers available for biosensor applications along with a generalized representation of how they function in analyte detection. Of these types of biosensors, the most commonly employed, due to the relative simplicity and low cost of its implementation, is the enzyme-based electrochemical biosensor [6].

Enzyme-based electrochemical biosensors are typically constructed by simply modifying an appropriate electrode with the enzyme of choice. In some cases, the electrode is also modified with an additional element such as a coenzyme. The highly selective enzyme catalyzes the conversion of the analyte into a species that is more readily detected than the analyte itself. Depending on the chemical properties of the species produced by the enzyme, there are two electroanalytical techniques that can be used for its detection: potentiometric and amperometric.

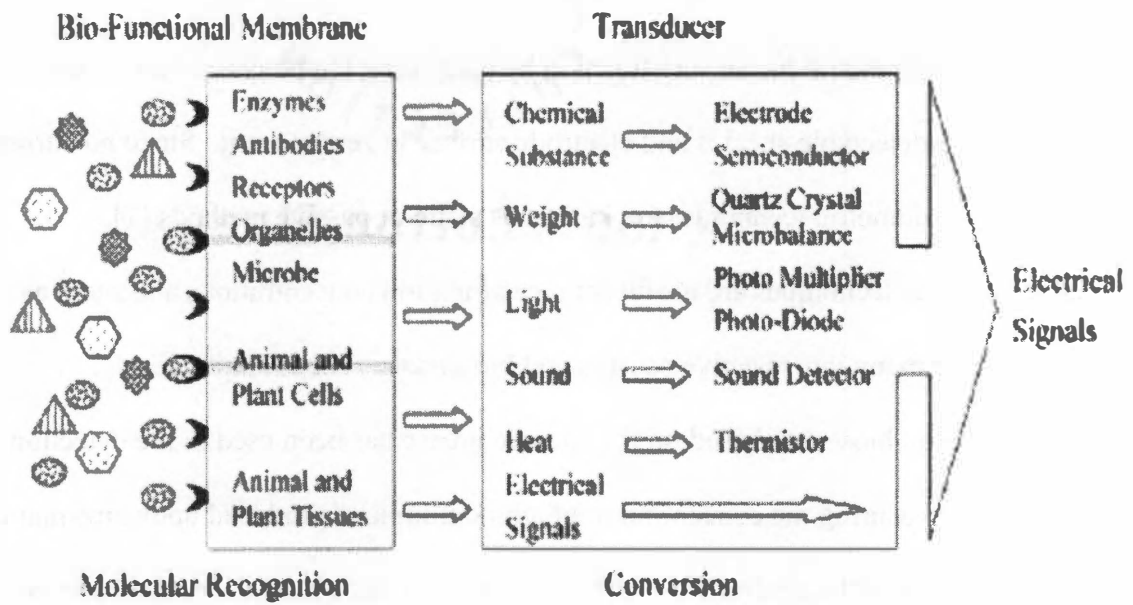


Figure 2.1: The different kinds of biological elements and transducers used in biosensors and the general principles of how they function.

Source: Nakamura H and Karube I (2003) *Anal. Bioanal. Chem.* 377: 446-468.

Potentiometric biosensors function by measuring the potential that exists between the detectable species and electrode surface at zero current. Since no current flows, potentiometric techniques are known as static or passive methods [7].

Potentiometric techniques are useful for measuring ion concentrations and serve as the basis for many ion-selective sensors and biosensors. For example, a potentiometric biosensor based on the enzyme urease has been used in the detection of urea by measuring the concentration of ammonium ions produced upon enzymatic decomposition of the analyte [8]. Although potentiometric biosensors have proven useful in situations where ions are involved, in many cases ions are not available for quantifying analyte concentrations.

Amperometric techniques, also known as dynamic methods, provide a solution to the limitations of potentiometric techniques. In contrast to potentiometric biosensors, amperometric biosensors function by measuring the current that flows between the detectable species and electrode surface at constant potential [7]. The current flows as a result of redox reactions involving the detectable species. Thus, many redox-active species can be detected using amperometric techniques, provided that the electrode material is conducive to electron transfer and the potential of the electrode relative to a reference electrode is maintained near the oxidation or reduction potential of the species being detected. The versatility of amperometric techniques has led to the development of many enzyme-based amperometric biosensors capable of detecting a wide variety of analytes.

2.1 Fundamentals of Enzyme-based Amperometric Biosensors

As mentioned in the previous section, amperometric techniques are used to quantify analyte concentrations by measuring the current generated at constant potential by redox reactions occurring at the electrode surface. The electrode at which the analyte or detectable species undergoes a redox reaction is called the *working electrode*. There are many varieties of working electrodes which differ in their geometries, surface characteristics and materials of construction. The working electrode is held at a constant potential relative to a *reference electrode*. Common reference electrodes include the Ag/AgCl electrode and the standard calomel electrode (SCE). In addition to the working and reference electrodes, a third electrode, called the *auxiliary electrode*, is required to complete the circuit. Frequently, a platinum wire is used for the auxiliary electrode. All three electrodes are typically placed together in an *electrochemical cell* and submersed in a solution containing the analyte [7]. The potential between the working and reference electrodes is controlled by a *potentiostat*. The potentiostat functions by measuring the current flowing between the working and auxiliary electrodes and adjusting it to maintain a constant potential [9]. Figure 2.2 shows a schematic representation of a potentiostat and a three-electrode cell.

The mechanistic aspects of redox reactions occurring at the surface of the working electrode is an important issue in understanding how amperometric biosensors function and the factors affecting their performance. To address this issue,

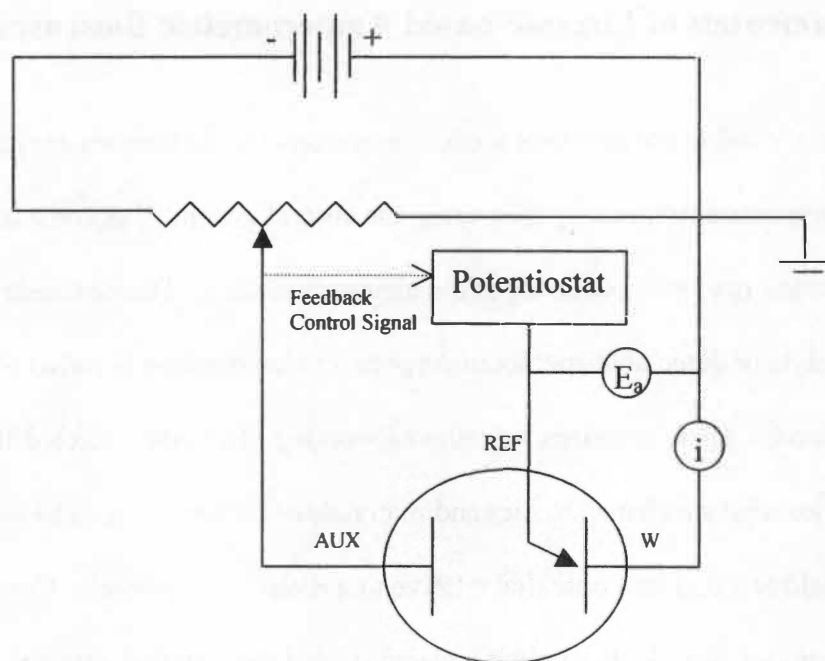


Figure 2.2: Schematic representation of a potentiostat and three-electrode cell.

Source: Kissinger PT and Heineman WH (1996) *Laboratory Techniques in Electroanalytical Chemistry*. 2nd Edition.

let us consider a hypothetical enzyme-based amperometric biosensor used in the detection of an analyte (A). The enzyme (E) and the oxidized form of its coenzyme (C_{ox}) are immobilized via covalent attachment and adsorption, respectively, on the surface of a planar working electrode. The enzyme-catalyzed reaction converts the analyte into a product (P) and the oxidized form of its coenzyme into the reduced form (C_{red}). Since the working electrode is held at or near the redox potential of the reduced coenzyme, as it is produced it is subsequently oxidized back to its original form. The current generated by oxidation of the coenzyme is measured by the internal ammeter of the potentiostat and used to quantify the concentration of the analyte. The working electrode of this hypothetical biosensor and the reactions occurring near its surface are shown in Figure 2.3.

At the atomistic level, analyte detection by an enzyme-based amperometric biosensor consists of three distinct steps, also shown in Figure 2.3. First, the analyte in the bulk solution must be transported to the surface of the working electrode by means of diffusion or forced-convection. Transport by diffusion can be described by Fick's law and is present in almost any amperometric measurement. Forced-convection refers to the movement of the solution by stirring the solution, rotating the electrode, or flowing the solution through the electrochemical cell. This transport method is often used to quickly carry analyte and product to and from the surface of the working electrode [7]. The second step in analyte detection is the enzyme-catalyzed reaction which converts the analyte into product(s). The kinetics of this

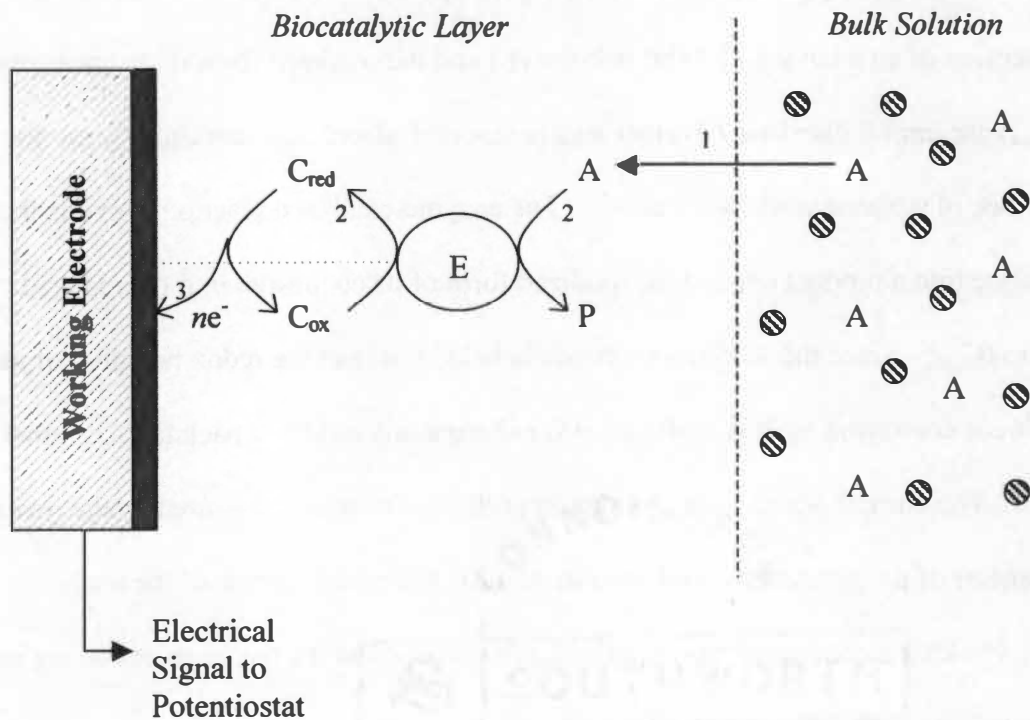


Figure 2.3: A hypothetical enzyme-based amperometric biosensor.

The grey dashed line connecting the working electrode to the enzyme represents the covalent attachment between the two. The steps labeled 1-3 represent the three steps involved with detection: 1. mass transport of analyte; 2. enzymatic reaction; 3. electron transfer between detectable species and working electrode. Note: The auxiliary and reference electrodes for this biosensor are not shown in this figure.

reaction are frequently described by the Michaelis-Menten equation for enzyme kinetics, shown below in Equation 2.1 [10]. The third and final step in analyte

$$v = \frac{v_m [S]}{K_m + [S]} \quad (2.1)$$

where, v = rate of reaction
 v_m = maximum rate of reaction
 $[S]$ = substrate concentration
 K_m = binding constant

detection is the transfer of electrons to/from the detectable species produced by the enzymatic reaction from/to the working electrode. The rate constant for electron transfer, denoted k^0 (cm/s), is typically determined experimentally and depends on the characteristics of the working electrode surface and the chemical species being oxidized or reduced [7]. The electron transfer rate constant is used in the Eyring equation, shown in Equation 2.2, to calculate the net current generated by oxidation and reduction of the detectable species [7].

$$i_{net} = nFAk^0 \left[C_O e^{-\alpha nF(E-E^{\circ'})/RT} - C_R e^{(1-\alpha)nF(E-E^{\circ'})/RT} \right] \quad (2.2)$$

where, i_{net} = net current
 n = number of electrons transferred
 F = Faraday's constant
 A = electrode surface area
 k^0 = electron transfer rate constant
 C_O = concentration of oxidized species
 C_R = concentration of reduced species
 α = electron transfer coefficient
 E = applied potential
 $E^{\circ'}$ = formal potential
 R = Gas constant
 T = temperature

Each of the three steps described above can be rate-determining under the appropriate conditions. For example, choosing a working electrode material that exhibits a relatively low k^0 might cause the electron transfer step to become rate-determining. Identifying which step is rate-determining is an important objective in designing and evaluating the performance of amperometric biosensors. It is almost always desirable to have the transport of analyte to the electrode be the rate-determining step as it leads to the most reliable measurements and extends the concentration range of accurate analyte detection [6]. We will return to this issue later in the text and discuss it in greater detail.

2.2 Designing Enzyme-based Amperometric Biosensors

When designing an enzyme-based amperometric biosensor, there are a number of issues that must be considered in order to optimize its performance. Obviously, since biosensors are often used *in vivo* in solutions that may contain numerous components, selectivity toward the analyte is of utmost importance in biosensor design. In addition, the biosensor must also possess high sensitivity and good operational stability under a variety of different operating conditions.

There are essentially three degrees of freedom in enzyme-based amperometric biosensor design: (1) the detectable, redox-active species, (2) the enzyme stabilization technique and (3) the working electrode material and its surface

characteristics. The choice of enzyme is not included as a degree of freedom here since it is usually dictated by the chemical properties of the analyte, although for some analytes there may be more than one enzyme that will suffice. However, the detectable species is a degree of freedom since coenzymes, reaction products, electron-mediators and in some cases, even enzymes themselves can effectively serve as the detectable species. As we will discover, the choice of detectable species is strongly correlated with the choice of working electrode material. The decisions made for each of the three degrees of freedom have a significant impact on the performance of a biosensor, and therefore, we will examine them all in more detail in the following sections.

2.2.1 Amperometric Detection of Redox-active Species

Enzymes from the class known as oxidoreductases are regularly used in enzyme-based amperometric biosensors due to their ability to catalyze redox reactions and produce redox-active products or coenzymes. There are a wide variety of oxidoreductases which differ in size, substrate specificity and functionality. The characteristics of a particular oxidoreductase chosen for use in a biosensor can help one decide on what type of detectable, redox-active species to employ for indirect analyte detection. The species commonly used for indirect analyte detection include reactants and products, coenzymes, enzymes and electron mediators.

When small oxidoreductases are used in biosensors, the enzyme itself can sometimes effectively serve as the detectable species. This is possible because the active site of

the enzyme is located close enough to its surface that direct electron transfer between the analyte and working electrode can occur. Horseradish peroxidase (HRP) is an excellent example of a small enzyme (MW 40 kDa) that is capable of mediating electron transfer. For example, Liu and Ju (2002) developed a hydrogen peroxide amperometric biosensor capable of direct electron transfer based on HRP immobilized on a colloidal gold-modified electrode [11]. Another example is the biosensor developed by Kong et al. (2003) which utilized HRP immobilized on a conducting polymer-modified electrode [12]. Figure 2.4 illustrates the process of direct electron transfer by HRP between an analyte and working electrode. Even for a small enzyme such as HRP, direct electron transfer is not always possible for biosensor applications, as the working electrode material and its surface characteristics have a significant impact on the ability of the enzyme to mediate electron transfer between the analyte and working electrode.

Most enzymes are too large and have their active sites buried too deeply within their structures for direct electron transfer to be a viable means of analyte detection. In such cases, detection is often accomplished through reactants, products, coenzymes or electron mediators. Glucose oxidase (GOD) is one particular enzyme for which all four of the previously mentioned detectable species have been used in the detection of glucose and these are shown in Figure 2.4. GOD catalyzes the oxidation of glucose with the aid of its coenzyme, flavin adenine dinucleotide (FAD), to gluconolactone and hydrogen peroxide. The first enzyme-based amperometric biosensors ever developed were based on GOD and detected glucose by measuring the decrease

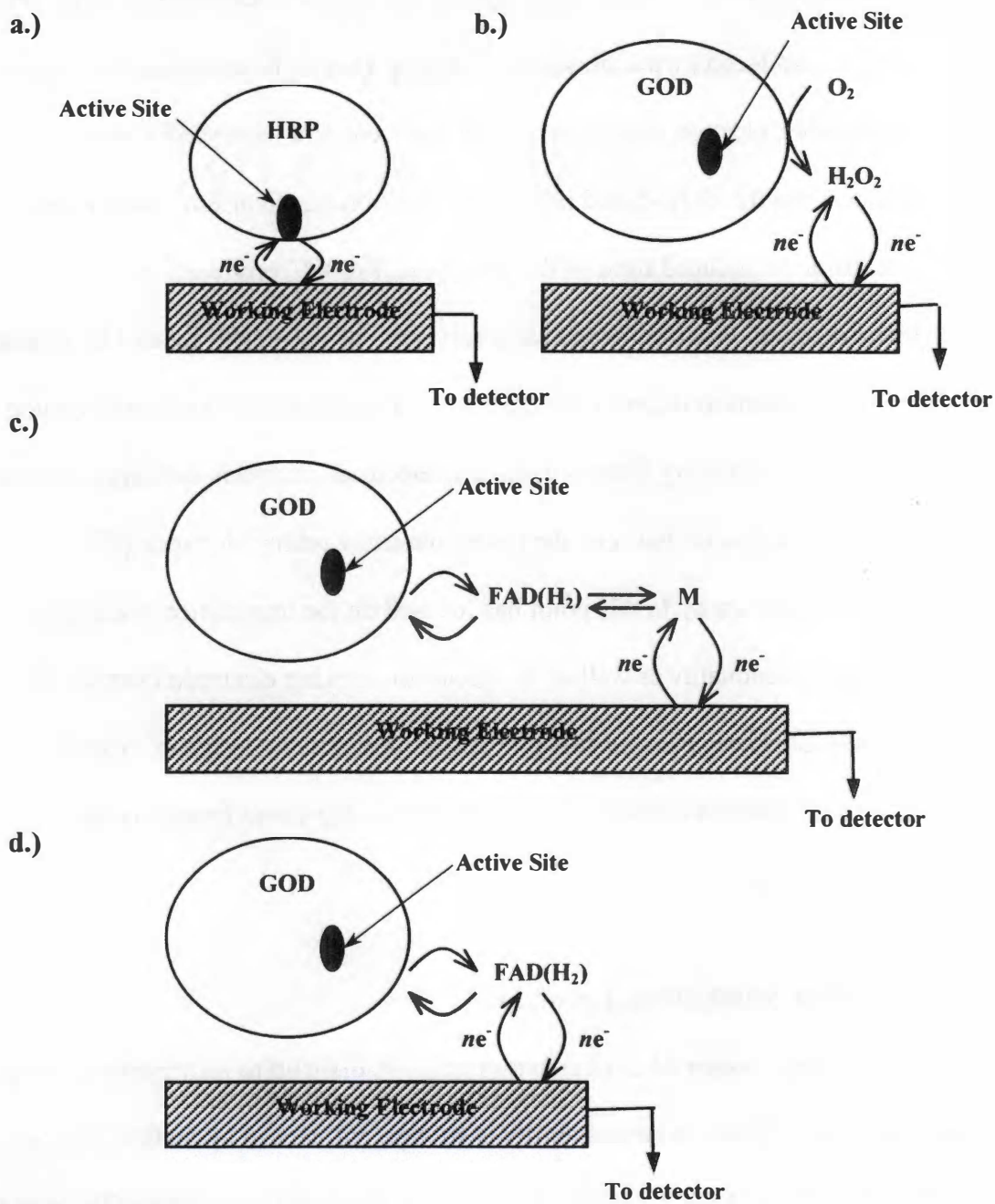


Figure 2.4: Examples of indirect analyte detection techniques.

(a) Direct electron transfer between analyte and working electrode by HRP, (b) detection of the reactant/product in the glucose oxidase (GOD)-catalyzed reaction, (c) detection of an electron mediator and (d) detection of the coenzyme.

in dissolved oxygen or the increase in hydrogen peroxide concentration as they were consumed or produced by the enzymatic reaction. Due to the complicated nature of these biosensors, electron mediators such as ferrocene and ferricyanide were incorporated into the GOD-based biosensor. Electron mediators are able to accept electrons from the reduced form of the coenzyme, FADH₂, produced by the enzymatic reaction. In turn, the mediator serves as the detectable species by donating its acquired electrons to the working electrode. An even simpler detection method was developed by utilizing advanced working electrode materials that were conducive to direct electron transfer between the coenzyme and working electrode [6].

The discussion up to this point has focused on the importance of enzyme structure and functionality as well as the choice of working electrode material in selecting a detectable species. While it is always desirable to design an optimal biosensor, compromises between the choices for the degrees of freedom must sometimes be made.

2.2.2 Enzyme Stabilization Techniques

The fragile nature of most enzymes makes it difficult to incorporate them into biosensors. In solution, enzyme stability is strongly influenced by factors such as temperature, pH and ionic strength. This is due to the tertiary structure of the active site, which is quite easily deformed when subjected to environmental conditions outside the stable range for the enzyme [13]. Active site deformation implies a loss of catalytic activity and this is what we would like to avoid in applying enzymes to

biosensors. To this end, enzyme stabilization techniques are used to increase the overall stability and reusability of enzyme-based biosensors.

One of the most effective means of stabilizing an enzyme is to immobilize it on a solid support; this is commonly accomplished through adsorption, entrapment or covalent attachment. The structural constraints placed on an immobilized enzyme serve to increase the stability of its tertiary structure. In addition, immobilization prevents leakage of an enzyme from the surface of a biosensor, thereby increasing its reusability. While there have been many studies done on the application of immobilization techniques to biosensors, we will focus our discussion on the more general aspects involved with employing these techniques.

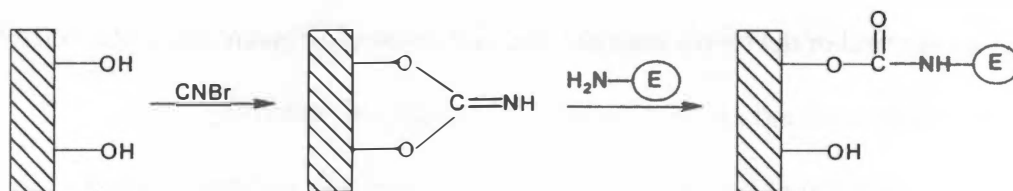
Adsorption of an enzyme to a solid surface is the simplest means of immobilization. Also, adsorption tends to be much less disruptive to enzyme structure than covalent techniques. However, the strength of binding forces between an enzyme and solid surface is susceptible to changes in pH, temperature and ionic strength. Some solid substrates commonly used for adsorption include alumina, charcoal, clay, cellulose, silica gel and collagen. Entrapment is an immobilization technique similar to adsorption in which an enzyme is physically confined within a solid or gel matrix. As expected, this technique possesses the same advantages and disadvantages of adsorption. An additional disadvantage of entrapment is the large diffusional barriers to the transport of substrate and product that exist as a result of the solid or gel matrix [6].

Covalent immobilization is often employed in applications where enzyme leakage is a major concern since the enzyme is anchored to a solid surface by means of a covalent attachment. As shown in Figure 2.5, a large variety of covalent attachment techniques have been developed which take advantage of the reactivities of different functional groups frequently found on enzymes and solid supports. These functional groups include amino, carboxylic acid, hydroxyl, phenolic, imidazole and thiol groups. The distance between the enzyme and support can in some cases be controlled by introducing a spacer molecule of the desired length into the immobilization process. The reactions involved with covalent attachment usually require specific conditions to proceed, and as a result, this technique is more difficult to implement than adsorption or entrapment. Another disadvantage of covalent attachment is that overall enzyme activity decreases because of the structural changes induced by the formation of covalent bonds [6].

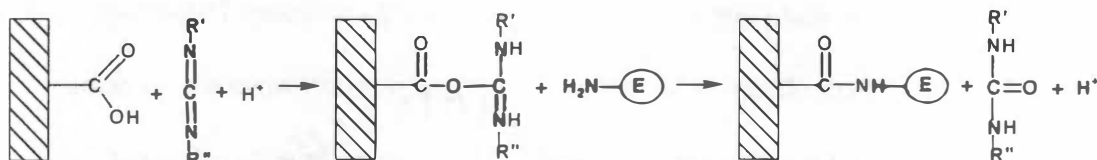
2.2.3 Working Electrode Materials

Perhaps the most important aspect of enzyme-based biosensor design is choosing an appropriate working electrode material. This is typically a difficult task as there are many varieties of materials and methods for modifying their surface characteristics that may be considered for a particular biosensor application. Accordingly, electrode materials have been the subject of intense research and great strides have been made in developing materials that have enabled the amperometric

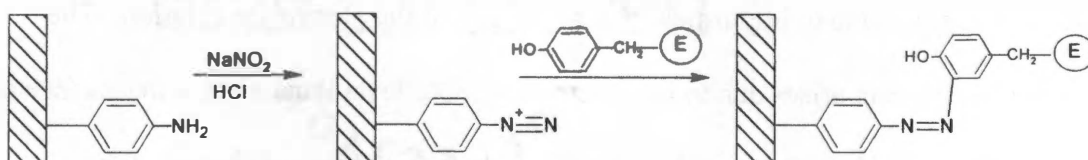
a) The cyanogen bromide technique



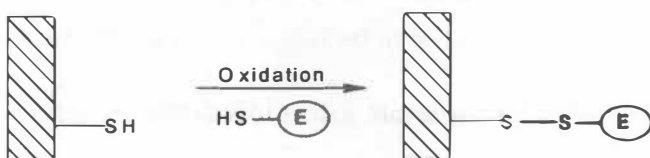
b) The carbodiimide technique



c) Coupling through diazonium groups from aromatic amino groups



d) Coupling via thiol groups



e) Coupling using cyanuric chloride

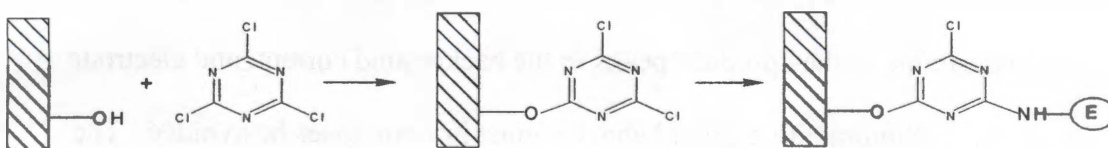


Figure 2.5: Common covalent immobilization techniques for enzymes.

Source: Turner APF, Karube I, Wilson GS (1987) *Biosensors: Fundamentals and Applications*.

detection of many new analytes. The ultimate goal in designing any enzyme-based biosensor is to find or develop a material that is conducive to electron transfer to/from the detectable species and exhibits optimal selectivity and sensitivity.

There are a couple of prerequisites that a prospective working electrode material should meet before receiving any further consideration. They are the background current and potential window of a working electrode. The background current is the current observed in a blank electrolyte solution when the working electrode is swept through a potential range. This current consists of several components including capacitive, redox reactions on the surface of the electrode and redox reactions due to impurities such as oxygen in the electrolyte solution. The capacitive current arises due to the electrical double-layer that exists at the surface of an electrode and is proportional to the electrode area and rate of change of the potential. The double-layer capacitance varies depending on the electrode material. Therefore, we should expect the background current to be larger for materials with a high double-layer capacitance and smaller for materials with a low double-layer capacitance. Redox reactions involving the surface of the electrode and impurities in the electrolyte solution also contribute to the background current. These components are undesirable as they produce peaks in the background current, and electrode materials exhibiting this type of behavior must in some cases be avoided. The potential window of a working electrode is defined as the potential range in which capacitive current is the main component of the background current. For biosensor applications, the working electrode potential is maintained near the redox potential of

the detectable species. Therefore, the working electrode material should be chosen such that the redox potential of the detectable species lies within the potential window of the electrode [7].

The most important requirement for a working electrode material is that it exhibits fast electron transfer kinetics such that low-potential analyte detection is possible. The rate of electron transfer depends on the physical properties and surface characteristics of the electrode material as well as the applied potential. The desirable physical properties of an electrode material are low electrical resistance, low porosity and high electrochemical inertness. As for the surface characteristics, it is desirable that the material have a high surface area and be as smooth as possible since surface roughness increases the background current. Another desirable characteristic is that the material be resistant to adsorption of the various compounds in solution as this has a detrimental effect on the electron transfer rate [7]. Many metal, carbon and polymer-based materials have been found to possess the physical properties and surface characteristics amenable to fast electron transfer kinetics and they have been used in numerous biosensor applications [1].

2.3 Evaluation of Enzyme-based Amperometric Biosensors

The first step in evaluating the performance of an enzyme-based biosensor is typically a cyclic voltammetry study. This type of study is also performed before the enzyme is applied to the electrode in order to obtain a qualitative measure of the

electron transfer rate constant between the electrode and detectable species. Cyclic voltammetry experiments are conducted in a quiescent electrolyte solution containing the detectable species. The current is measured as the working electrode potential is cycled through forward and then backward sweeps. Normally, the current exhibits two peaks (one for each sweep) corresponding to the oxidation and reduction potentials of the detectable species. If the kinetic rate of electron transfer to/from the working electrode is slow, we should expect to find the oxidation and reduction peak potentials shifted to more positive and negative values with respect to an electrode that exhibits a higher kinetic rate. Figure 2.6 shows a couple of hypothetical cyclic voltammograms for electrode materials with different kinetic rate constants. A thorough explanation of the theoretical and experimental aspects of cyclic voltammetry has been previously given by Kissinger and Heineman (1996) [7].

Once the peak redox potentials for the working electrode have been determined, the biosensor may be fully constructed and its performance evaluated in the detection of the analyte at the appropriate redox potential. The performance evaluation may consist of determining the linear concentration range of the biosensor, apparent enzyme kinetics, stability and reusability. The stability of the biosensor refers to the amount of degradation in the current produced at a particular analyte concentration observed over a period of time in which the biosensor is stored at certain conditions. The reusability refers to the number of repeated measurements the biosensor can make without losing a significant amount of its current response to the

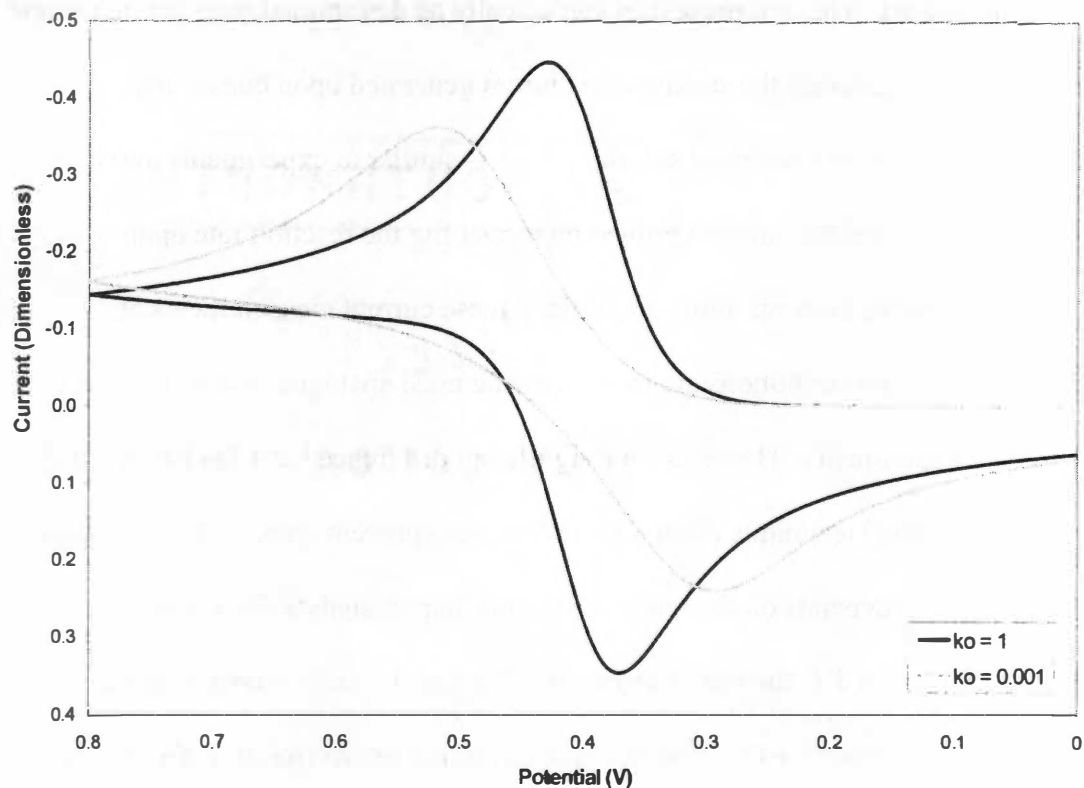


Figure 2.6: Hypothetical cyclic voltammograms for two materials.

These voltammograms show the effect of the electron transfer rate constant, k_0 , on the peak redox potentials of a detectable species. The scans were initiated at 0.0 V and swept to +0.8 V, then reversed and swept back to 0.0 V. The upper peaks represent oxidation of the species whereas the bottom peaks represent reduction.

analyte. The apparent enzyme kinetics and linear concentration range are slightly more complicated. The two properties can actually be determined together in a single experiment by measuring the steady-state current generated upon consecutive additions of analyte to the stirred solution. This is similar to experiments in which enzyme kinetic constants are determined by measuring the reaction rate upon increasing substrate concentration, and in fact, these current measurements at different analyte concentrations are the electrochemical analogue of direct enzyme kinetic rate experiments. However, one significant difference between the two is that the electrochemical technique often only reveals the apparent enzyme kinetics as the observed current depends on the rate-determining step in analyte detection. As discussed in section 2.1, the rate-determining step may be mass transport of the analyte to the electrode surface, the enzymatic reaction or electron transfer between the detectable species and electrode. The true enzyme kinetics will only be observed if the enzymatic reaction is the rate-determining step. Otherwise, the kinetics may be quite different from the true kinetics. For example, if electron transfer is rate-determining, the biosensor will show little or no response to increasing analyte concentration. The most desirable case from the point of view of an operating biosensor is that the mass transport step be rate-determining as this serves to increase the linear concentration range for the biosensor and is more reliable than electron transfer or enzymatic reaction rate-limited biosensors [6]. Figure 2.7 shows the enzyme kinetics and linear ranges observed for biosensors whose net reaction rates are determined by each of the three steps.

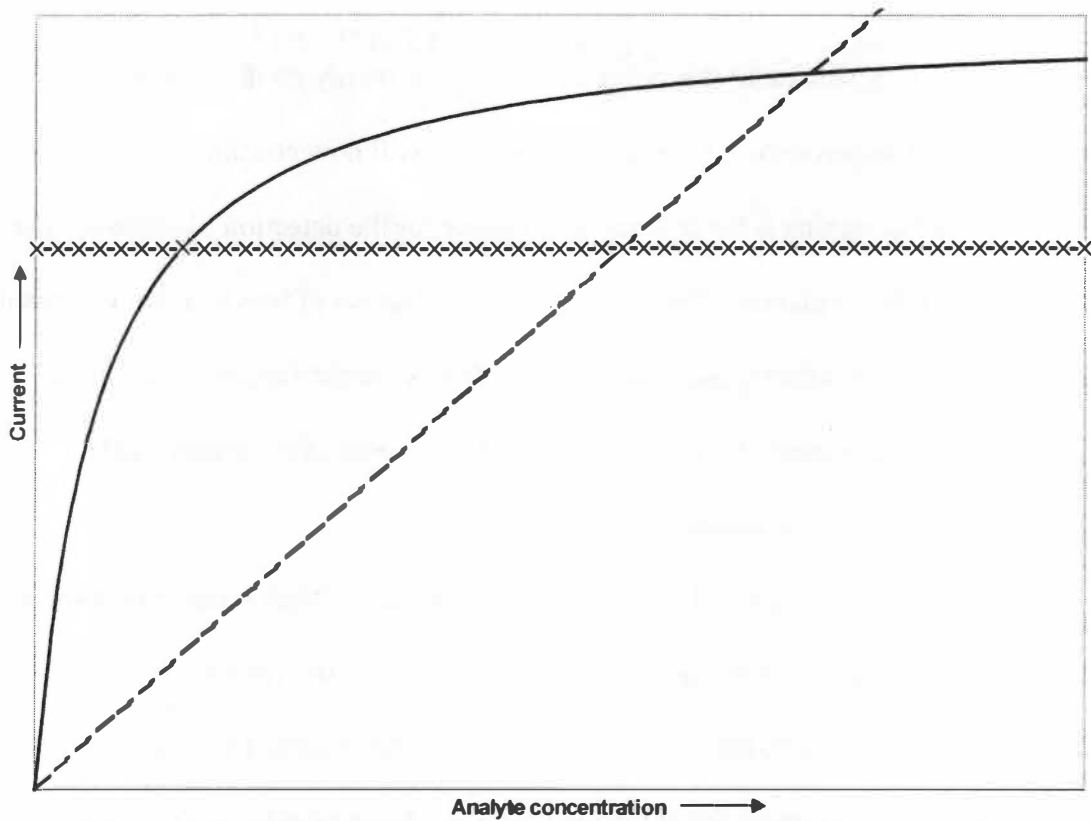


Figure 2.7: Apparent enzyme kinetics of a biosensor for different rate-determining steps.

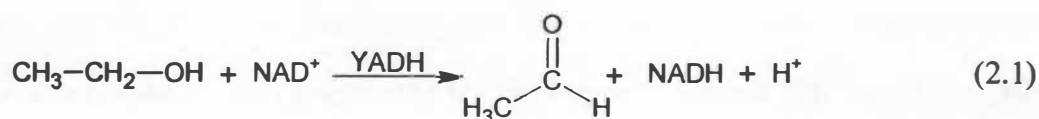
In this figure, the enzyme kinetics for a biosensor whose rate-determining step is the: mass transport (---), electron transfer (-X-) and enzymatic reaction (solid line) step.

Source: Turner APF, Karube I, Wilson GS (1987) *Biosensors: Fundamentals and Applications*.

2.4 Design Considerations for a YADH-based Biosensor

The discussion up to this point has focused primarily on the general aspects of enzyme-based amperometric biosensor design. We will now consider these aspects in the context of designing a YADH-based biosensor for the detection of ethanol. The emphasis will be on making choices for the design degrees of freedom that will result in an amperometric ethanol biosensor that exhibits better performance than those that have been previously developed. Table 2.1 lists some of these previously developed amperometric ethanol biosensors.

Before discussing the design considerations for a YADH-based biosensor, it may be helpful to understand the structure and function of the enzyme of interest, YADH. YADH is an oxidoreductase produced by Baker's yeast (*Saccharomyces cerevisiae*) which catalyzes the oxidation of ethanol to acetaldehyde with the aid of the coenzyme, NAD^+ , as shown in Equation 2.1. The molecular weight of the



enzyme is approximately 140 kDa and its structure consists of four identical subunits which each contain an active site [14]. The active site contains a zinc atom which is critical to catalytic activity as the substrate and coenzyme are positioned near it such that electron transfer between the two becomes more thermodynamically favorable. The enzyme is extremely specific toward ethanol and binds it strongly. The binding

Table 2.1: Examples of previously developed enzyme-based amperometric ethanol biosensors.

Enzyme	Working Electrode Material	Detected Species	Linear Concentration Range	Ref.
YADH	Carbon Paste	Mediator	50 μ M - 1 mM	15
YADH	Carbon Paste	Mediator	45 μ M - 4 mM	16
YADH	Carbon Felt	Mediator	0.2 mM - 5 mM	17
YADH	Carbon Paste	Mediator	0.1 mM - 20 mM	18
YADH	Chemically-modified Carbon Paste	NADH	0.03 μ M - 3 μ M	19
YADH	Carbon Nanotube/Teflon	NADH	< 1 mM	20
YADH	Chemically-modified Polymer	NADH	0.3 mM - 1 mM	21

constant, K_m , for ethanol has been determined to be about 17 mM at pH 7.3 and 30°C [22]. The enzyme can bind other primary alcohols as well, although not as strongly as ethanol. Compared to its mammalian counterpart, YADH is larger and more complex and is about 100 times more active [23]. The large catalytic activity of YADH makes it desirable for use in ethanol biosensors.

2.4.1 Amperometric Detection of NADH

There are many enzymes which utilize NAD^+ or its reduced form NADH in catalyzing redox reactions. Consequently, significant effort has been devoted to developing amperometric detection techniques for both forms of the coenzyme. The goals of this effort have been to find materials which exhibit fast electron transfer kinetics to/from the coenzyme and to preserve the coenzyme against electrochemical degradation so that it can be reused many times in a biosensor and does not foul the surface of the working electrode.

The amperometric reduction of NAD^+ to NADH has proven to be extremely difficult because of its tendency to form inactive dimers when electrochemically reduced [24]. Some progress has been made, however, by using electrodes modified with an electron transfer mediator [25, 26]. The amperometric oxidation of NADH to NAD^+ , while much easier to achieve than the former case, has some challenges that need to be overcome as well. The main problem encountered in NADH oxidation has been slow electron transfer kinetics which require high overpotentials to achieve detection. High overpotentials are undesirable in amperometric biosensors as they

significantly decrease their sensitivity and selectivity [27]. Not surprisingly, the early efforts in amperometric NADH oxidation focused on using electron transfer mediators to reduce the oxidation overpotential. Some mediators that have been effectively employed include potassium hexacyanoferrate, Meldola's Blue, dichlorophenolindophenol, *p*-benzoquinone, *o*-phenylenediamine and 3,4-dihydroxybenzaldehyde. These mediators have been used in solution, adsorbed or covalently attached to the electrode surface and electropolymerized on the electrode surface [27]. More recently, electrode materials have received a great deal of attention in developing biosensors which are capable of directly oxidizing NADH. In particular, electrodes modified with carbon nanomaterials have been shown to enable low potential NADH oxidation.

2.4.2 Carbon Nanomaterials as Working Electrode Materials

The physical properties of carbon nanomaterials such as nanotubes and nanofibers make them attractive for incorporation into amperometric biosensors. Their high surface areas and electrical conductivities are amenable to fast electron transfer kinetics and low potential analyte detection [28]. Carbon nanotubes (CNTs) and nanofibers (CNFs) are physically similar materials except that nanofibers are typically have much larger diameters and possess many more surface defects than nanotubes. There are a variety of methods for preparing CNTs and CNFs including laser ablation, arc discharge and chemical vapor deposition. The first two methods are frequently used to produce single-walled carbon nanotubes (SWNTs), whereas the

chemical vapor deposition method is used to produce multi-walled carbon nanotubes (MWNTs) and CNFs [29, 30]. Figure 2.8 shows a carpet of CNFs grown on a silicon support using the chemical vapor deposition method [31]. The production and purification of SWNTs and MWNTs is more complicated than that of CNFs, and as such, they are typically more expensive. Most of the research work has focused on applying CNTs to the working electrodes of biosensors. However, CNFs are promising working electrode materials as well and deserve further investigation.

There have been many studies performed on incorporating SWNTs and MWNTs into amperometric enzyme-based biosensors. For example, Xu et al. (2003) developed a hydrogen peroxide biosensor based on the enzyme HRP and the mediator Methylene Blue by depositing them on the surface of a glassy carbon electrode modified with a thin layer of MWNTs [32]. This biosensor was reported to exhibit exceptional performance in detecting hydrogen peroxide. Direct electron transfer between HRP and MWNTs has also been shown to be an effective means of hydrogen peroxide detection [33]. For the detection of glucose, Wang et al. (2003) fabricated a gold-MWNT electrode doped with GOD which showed much better performance than a glassy carbon electrode [34]. An example more relevant to this study is the MWNT-teflon/YADH/NAD⁺ composite electrode developed by Wang and Musameh (2003) for use in the detection of ethanol [20]. This biosensor enabled the direct detection of NADH at much lower potentials than a graphite-based biosensor.

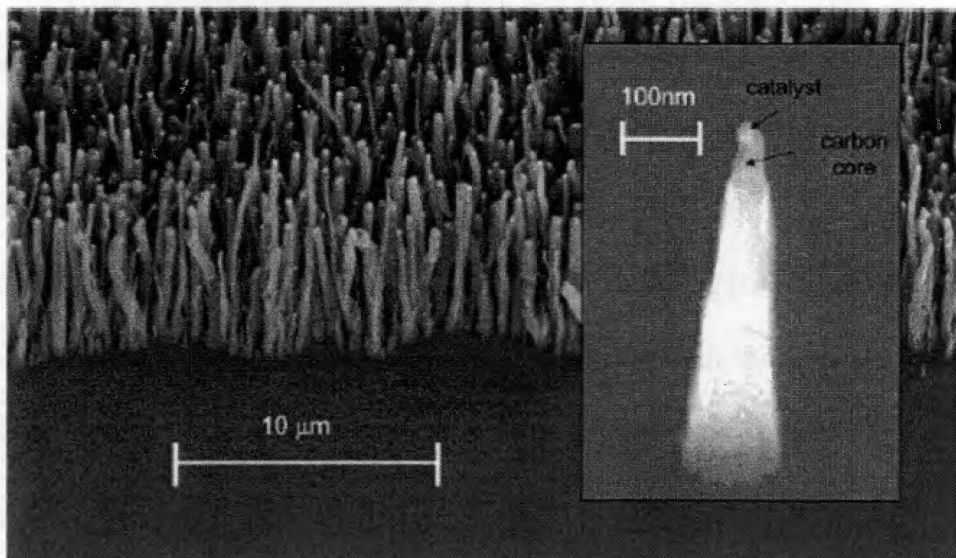


Figure 2.8: Scanning electron micrograph of CNFs grown on a silicon support.

Source: McKnight et al. (2003) *J. Phys. Chem. B* **107**: 10722-10728.

While CNTs have been studied extensively as working electrode materials for amperometric biosensors, to the author's knowledge there have been no such studies performed for CNFs. However, there have been a few studies which evaluated the effectiveness of using CNFs as a working electrode material for the amperometric detection of various redox-active species. Murphy et al. (2003) reported that a porous ceramic-CNF electrode exhibited good electrochemical behavior in the oxidation of hydroquinone and phenol [35]. Another study by Marken et al. (2001) examined the redox behavior of various metals at porous and non-porous CNF electrodes [36]. These results suggest that CNFs might be able to serve as good working electrode materials for amperometric biosensors.

2.4.3 YADH Immobilization on Carbon Nanomaterials

Enzymes can be immobilized on CNTs and CNFs via adsorption or covalent attachment. In either case, the materials are typically subjected to an oxidation treatment prior to immobilization. The oxidation treatment introduces oxygen-containing functionalities at the defect sites on the surface of CNTs and CNFs. These surface functionalities may serve as enzyme attachment points in a covalent immobilization scheme. For example, Huang et al. (2002) covalently immobilized bovine serum albumin on MWNTs by linking lysine residues on the protein to carboxylic groups on the surface of the nanotubes [37]. This immobilization technique utilized 1-ethyl-3-(3-dimethylaminopropyl)carbodiimide (EDAC)-activated

amidation to covalently attach the enzyme, as shown in Figure 2.9. With regard to YADH immobilization, EDAC-activated amidation is a good choice for covalent attachment as the enzyme contains many lysine residues near its surface that can be linked to surface carboxylic groups using this technique.

2.4.4 Design Proposal for a YADH-based Biosensor

It is proposed to develop and evaluate the performance of several YADH-based biosensor designs. Detection of ethanol will be achieved by direct oxidation of NADH at the working electrode. Thin films of MWNTs and CNFs will be applied to a glassy carbon working electrode and each material evaluated in its effectiveness at analyte detection. In addition, YADH will be adsorbed and covalently attached to the surface of the modified working electrodes to determine the effects of the immobilization technique on the stability and reusability of the biosensor. The performance of these biosensors will be compared to previously developed ethanol biosensors as well as a graphite-based ethanol biosensor that will also be constructed.

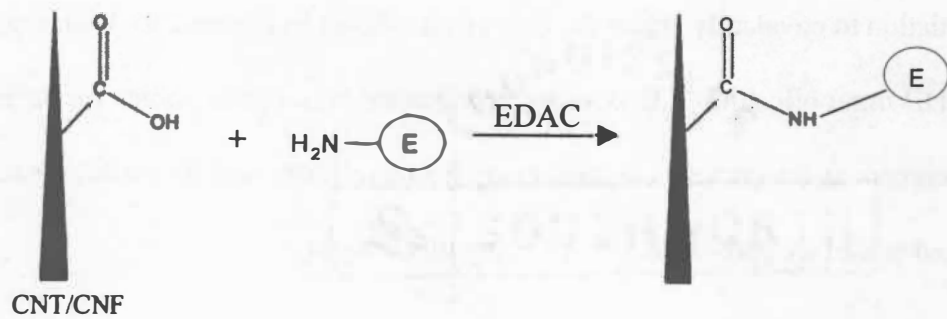


Figure 2.9: Covalent attachment of an enzyme to CNTs/CNFs via EDAC-activated amidation.

CHAPTER 3 MATERIALS AND METHODS

3.1 Reagents

Yeast alcohol dehydrogenase (YADH, 400 U/mg), oxidized and reduced nicotinamide adenine dinucleotide (NAD^+/NADH), N-hydroxylsuccinimide (NHS) and 1-ethyl-3-(3-dimethylaminopropyl)carbodiimide (EDAC) were obtained from Sigma (Sigma-Aldrich Corp., St. Louis, MO). Ethanol (200 proof USP) and powdered graphite were obtained from Fisher (Fisher Scientific, Hampton, NH). Multi-walled nanotubes (MWNTs) with an average OD of 15 nm and length of 5-20 μm were supplied by NanoLab in powder form (NanoLab Inc., Newton, MA). Carbon nanofibers (CNFs) with an OD of 100-200 nm and length of 30-100 μm were also supplied in powder form by Applied Sciences (Applied Sciences Inc., Cedarville, OH). Both the MWNTs and CNFs were produced via the chemical vapor deposition process. All other chemicals were of analytical grade. All solutions were prepared using deionized water.

3.2 Apparatus

The electrochemical measurements were conducted using a computer-controlled CHI660A (CHI Company) potentiostat. The working electrode was a 3.0 mm diameter planar surface glassy carbon (GC) electrode obtained from Bioanalytical Systems (BAS, model MF-2012). The reference electrode was an Ag/AgCl electrode (BAS, model RE-5B) and the auxiliary electrode was a platinum

wire (BAS, model MW-4130). All three electrodes were inserted through holes in a Teflon cap into a 10 ml electrochemical cell. A magnetic stir bar placed in the cell provided convective transport during amperometric measurements.

A Beckman UV/Vis spectrophotometer (model DU 500) was used to quantify the surface coverage of YADH on the working electrode. Absorbance measurements were performed at a wavelength of 340 nm in a quartz cuvette with a 1 cm path length.

3.3 Fabrication of the Ethanol Biosensor

Prior to use, the MWNTs and CNFs were separately subjected to an oxidation treatment by refluxing them in 3 M HNO₃ for 48 h [38]. After the oxidation treatment, the suspensions were vacuum-filtered through a Whatman 0.02 μm Apodisc[®] membrane filter and then rinsed with deionized water until the filtrate reached neutral pH. The MWNTs and CNFs were then collected into separate glass vials and placed in a drying oven at 80°C for 24 h. Once dry, the materials were solubilized using different techniques. The MWNTs were solubilized by placing 1 mg of the oxidized material into 10 mL of 0.02 M sodium dodecyl sulfate (SDS) and sonicating for several minutes. The CNFs were solubilized in the same manner except that acetone was used as the solvent. In both cases, the resulting solutions were opaque and homogeneous in appearance. An additional solution was prepared by placing 1 mg of pristine graphite powder in 10 mL of acetone and briefly sonicating.

The surface of the glassy carbon working electrode was polished with an 0.05 μm alumina slurry on a Texmet polishing pad. The electrode was then thoroughly rinsed with deionized water, briefly sonicated, rinsed again and allowed to dry under ambient conditions. Next, the electrode surface was modified with a thin film of MWNTs, CNFs or graphite by depositing 10 μL of the solution on the surface and allowing the solvent to evaporate under vacuum. After drying, the electrode was rinsed with deionized water.

The procedure for incorporating YADH into the modified electrode varied depending on which immobilization technique was employed. For adsorption, 10 μL of 1 g/L YADH in pH 7.4 phosphate buffered saline (PBS) was deposited on the modified electrode surface and dried under vacuum. The procedure for covalent attachment consisted of several steps. First, 10 μL of 5 g/L EDAC in pH 6.0 2-(N-morpholino)ethanesulfonic acid (MES) and 10 μL of 5 g/L NHS in pH 6.0 MES were deposited simultaneously on the electrode surface and allowed to dry under vacuum. Next, the electrode was rinsed with deionized water and 10 μL of 1 g/L YADH was deposited on the surface. After drying under vacuum, the electrode was again rinsed with deionized water. In both immobilization techniques, the final step was to deposit 10 μL of 5 mM NAD^+ in pH 7.4 PBS on the electrode, dry under vacuum and rinse with deionized water. The procedure for depositing the enzyme and coenzyme on the modified electrode separately was derived from the work of Xu et al. (2003) [32].

CHAPTER 4 RESULTS AND DISCUSSION

4.1 Electrochemical NADH Oxidation at Graphite-, CNF- and MWNT-modified GC Electrodes

The first amperometric measurements were performed on the GC electrode modified with MWNTs, CNFs and graphite to assess the electron transfer kinetics between the working electrode material and NADH. In each case, the working electrode was prepared as described above except that the enzyme and coenzyme were not incorporated into the electrode. The working, reference and auxiliary electrodes were submersed in a quiescent solution of 1 mM NADH in pH 7.4 PBS and measurements were made using cyclic voltammetry (CV). All CV scans were performed under identical conditions; the potential was scanned from -0.10 V to $+0.80$ V (vs. Ag/AgCl) and then scanned back to the starting potential. Due to the difficult nature of electrochemical NAD^+ reduction (as discussed previously), the cyclic voltammograms do not exhibit a reduction peak on the reverse scan.

Figure 4.1 shows the cyclic voltammogram for NADH oxidation at an unmodified GC electrode along with its background current in pH 7.4 PBS. As can be seen in this figure, the peak potential for NADH oxidation occurs at $+0.68$ V. For comparison, Musameh et al. (2002) reported a peak potential of $+0.82$ V (vs. Ag/AgCl) for NADH oxidation at an unmodified GC electrode [39]. The cyclic voltammogram for the graphite-modified GC electrode, shown in Figure 4.2, exhibits

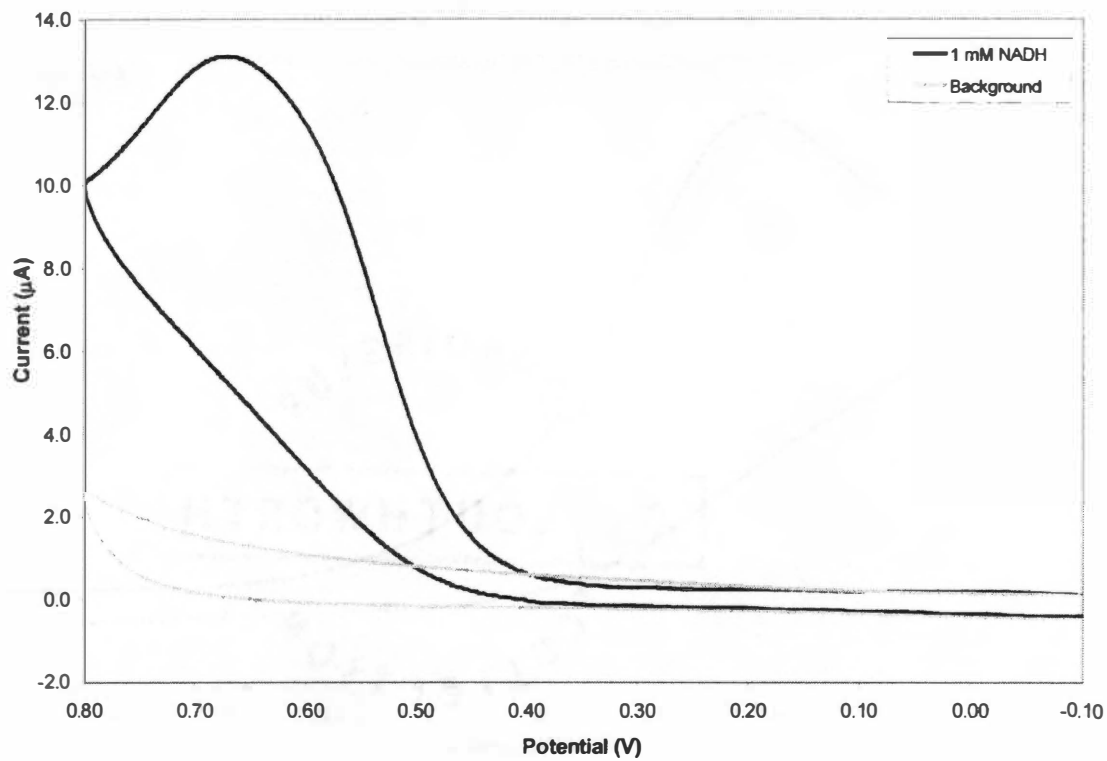


Figure 4.1: Cyclic voltammogram for an unmodified GC electrode in 1 mM NADH.

The supporting electrolyte was pH 7.4 PBS and the scan rate was 100 mV/s.

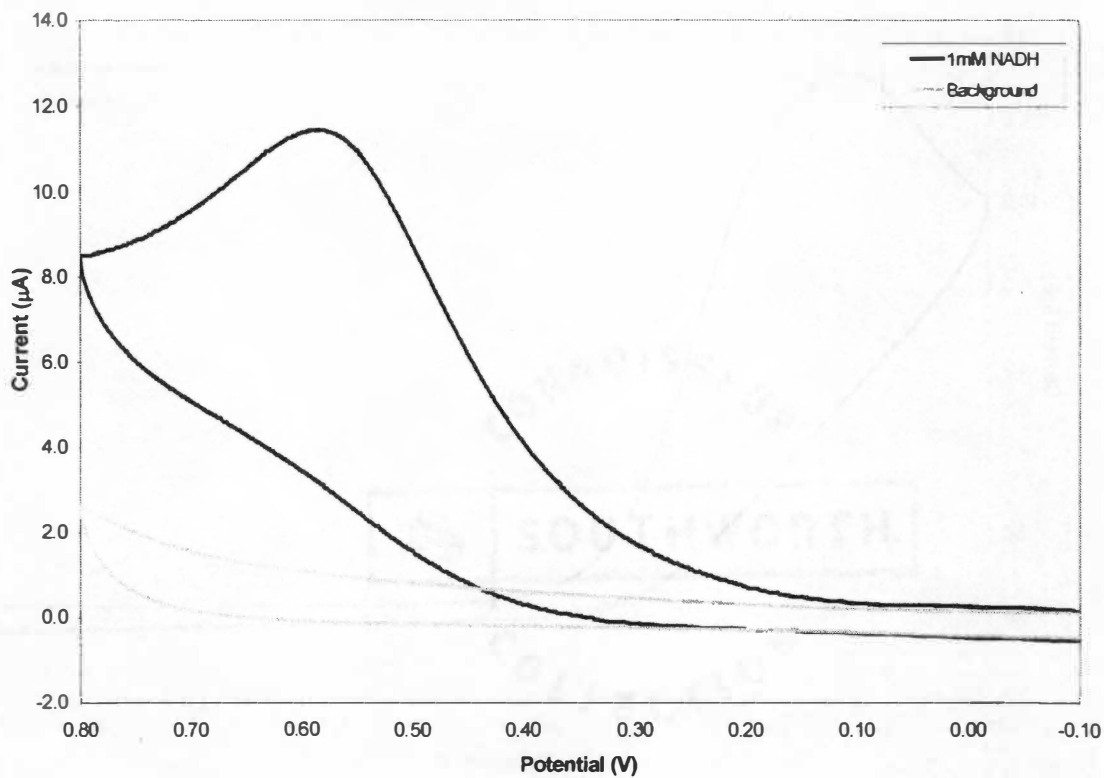


Figure 4.2: Cyclic voltammogram for a graphite-modified GC electrode in 1 mM NADH.

The supporting electrolyte was pH 7.4 PBS and the scan rate was 100 mV/s.

a slightly lower NADH peak oxidation potential of +0.60 V compared to the unmodified GC electrode. The electrode also has a relatively small background current in pH 7.4 PBS. The voltammogram for the CNF-modified electrode in Figure 4.3 indicates a peak oxidation potential of +0.64 V, which suggests that the electron transfer kinetics of CNFs are similar to that of graphite. Finally, the voltammogram for the MWNT-modified electrode is shown in Figure 4.4. Clearly, this electrode exhibits markedly different behavior than those previously discussed. The most important difference is the significant shift in the peak oxidation potential to +0.43 V. In addition, the peak is much broader and the background current larger than that observed for the other electrodes. Figure 4.5 shows the cyclic voltammograms for all of the electrodes.

The modified GC electrodes were also characterized by performing amperometric NADH detection experiments. The electrochemical cell was initially charged with 6 ml of pH 7.4 PBS and stirred magnetically at 400 rpm. The electrodes were inserted into the solution and a potential of +0.2 V was applied between the working and reference electrodes. Once the transient current had decayed, the detection experiment was initiated by making 0.1 ml additions of 1 mM NADH to the solution in 20 s intervals. The current generated by oxidation of NADH at the constant potential was measured and recorded. This experiment was performed for the graphite-, CNF- and MWNT-modified GC electrodes and the results are shown in Figure 4.6. As expected from the results of the cyclic voltammetry experiments, the MWNT-modified GC electrode was found to exhibit a much larger response to

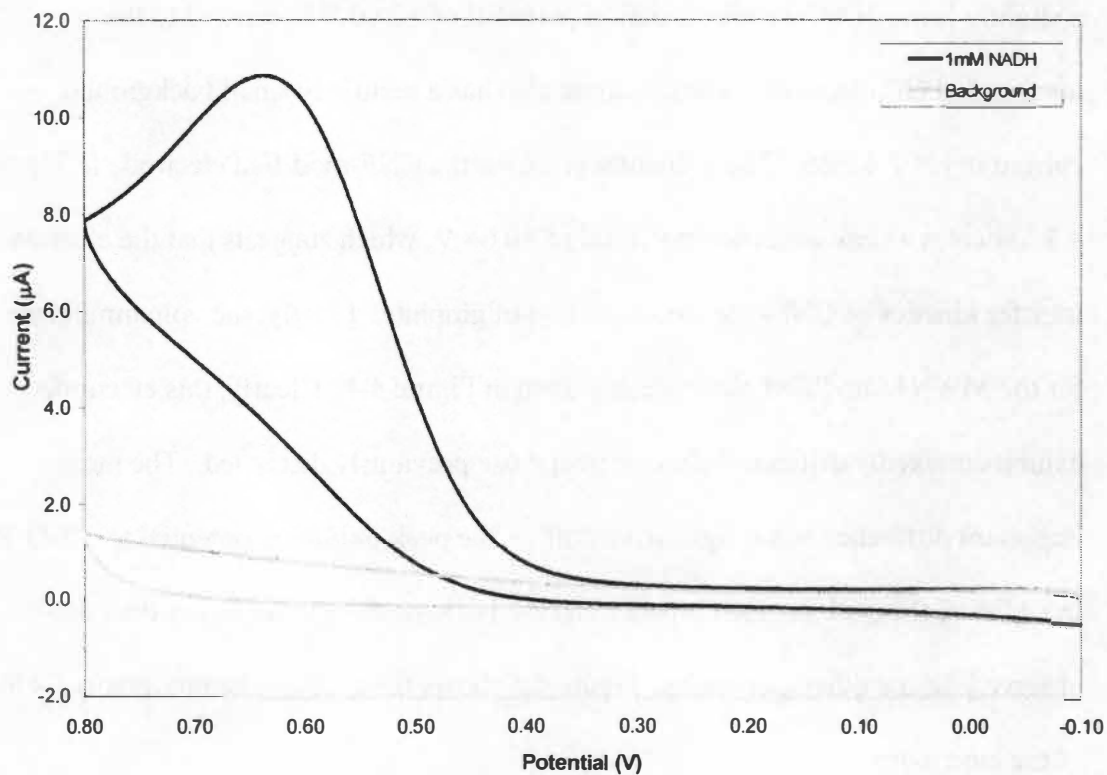


Figure 4.3: Cyclic voltammogram for a CNF-modified GC electrode in 1 mM NADH.

The supporting electrolyte was pH 7.4 PBS and the scan rate was 100 mV/s.

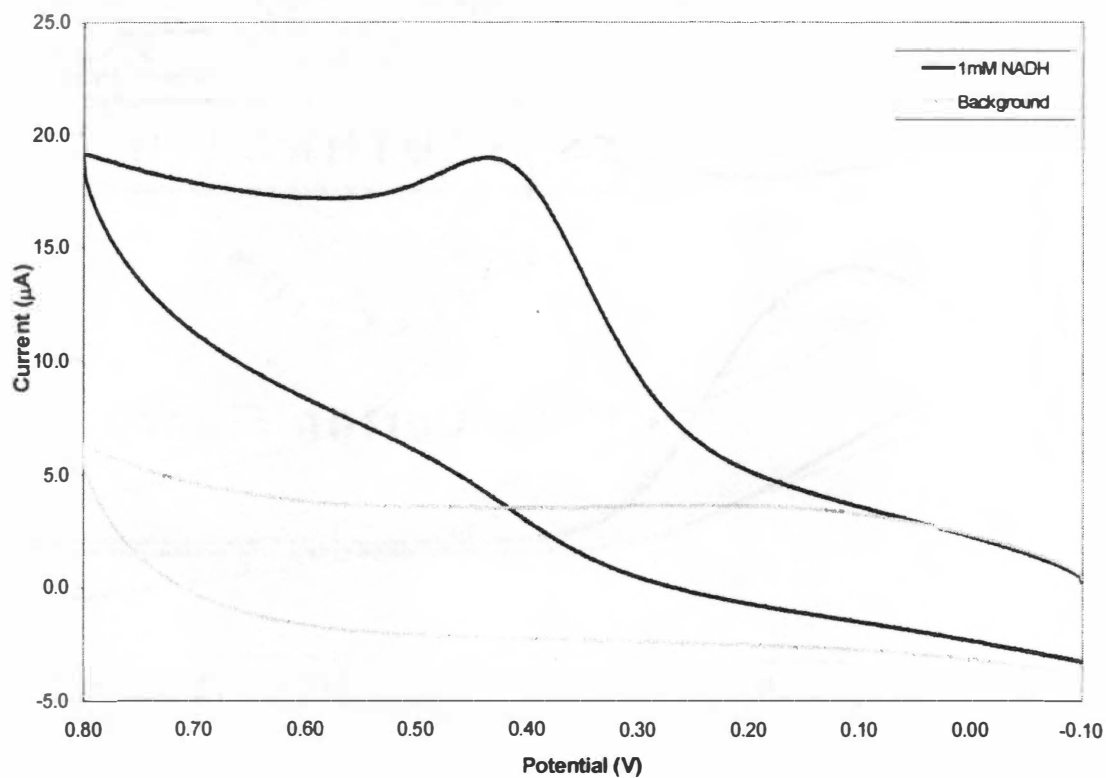


Figure 4.4: Cyclic voltammogram for a MWNT-modified GC electrode in 1 mM NADH.

The supporting electrolyte was pH 7.4 PBS and the scan rate was 100 mV/s.

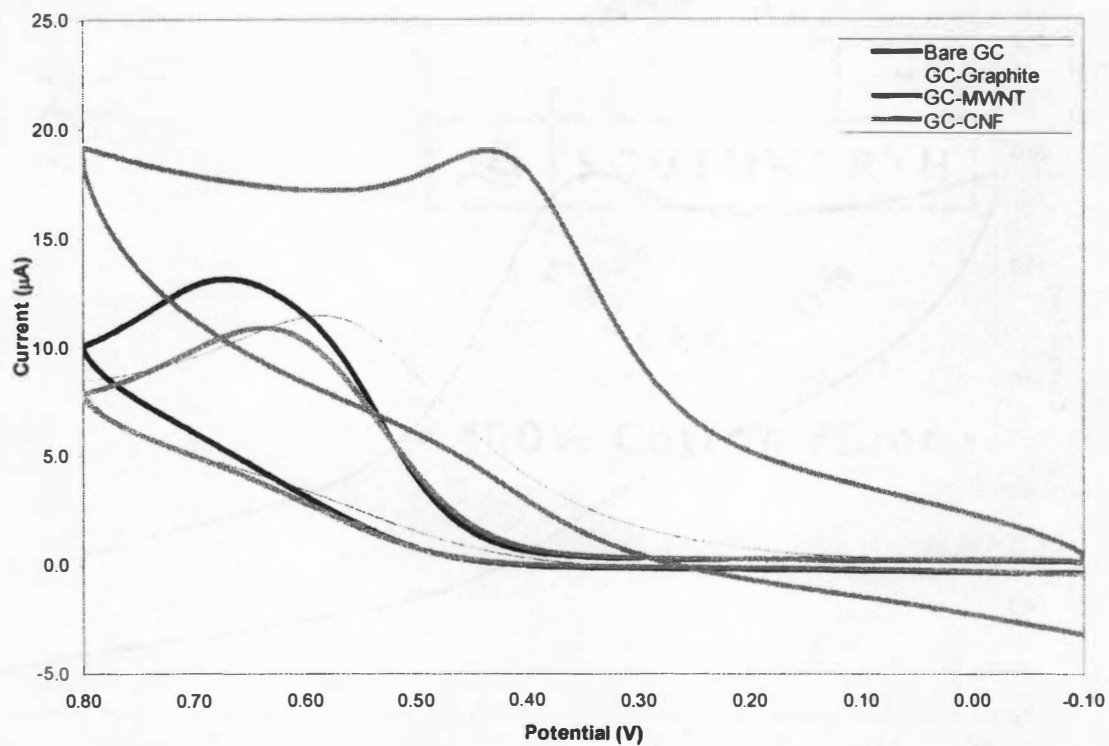


Figure 4.5: Cyclic voltammograms for unmodified, graphite-, CNF- and MWNT-modified GC electrodes in 1 mM NADH.

The supporting electrolyte was pH 7.4 PBS and the scan rate was 100 mV/s. The background voltammograms are not shown in this figure.

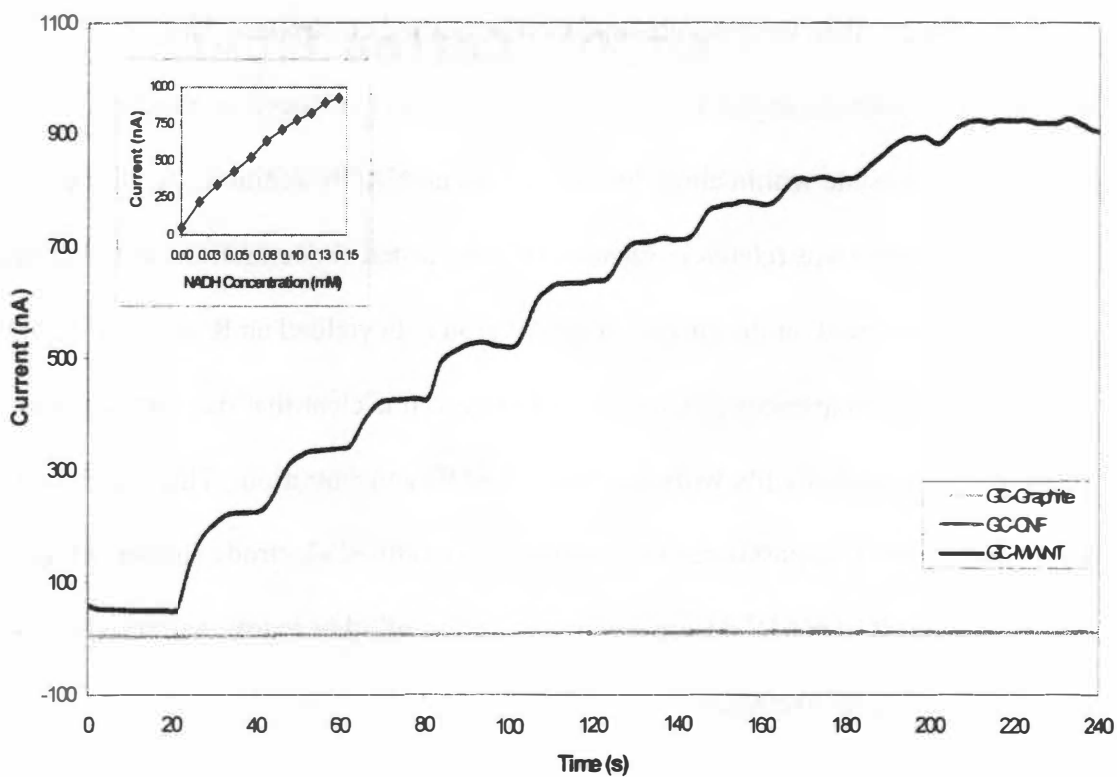


Figure 4.6: Amperometric detection of NADH at graphite-, CNF- and MWNT-modified GC electrodes.

The supporting electrolyte was pH 7.4 PBS. The solution was magnetically stirred at 400 rpm and the working potential was +0.2 V. The inset shows the current as a function of NADH concentration for the MWNT-modified GC electrode.

NADH at +0.2 V than the graphite- and CNF-modified electrodes. The MWNT-modified electrode displayed a quick response time, as evidenced by the current reaching steady-state within about ten seconds of an NADH addition. Also, the electrode response was relatively linear within the tested concentration range; a linear regression performed on the current-concentration data yielded an R^2 value of 0.9815 (Figure 4.6 inset, regression not shown). However, it is clear that the magnitude of the response decays slightly with increasing NADH concentration. This phenomenon might be attributed to passivation of the MWNT-modified electrode surface which occurs as a result of NAD^+ adsorption or adsorption of other redox-inactive species produced by NADH oxidation.

4.2 Electrochemical Ethanol Detection by Graphite-, CNF- and MWNT-based Biosensors

After characterizing the behavior of the modified electrodes toward NADH, fabrication of the biosensors was completed by incorporating YADH and NAD^+ into the graphite-, CNF- and MWNT-modified electrodes. Amperometric ethanol detection experiments were then performed in a manner similar to that used for NADH detection. The electrochemical cell was initially charged with 3 ml of pH 7.4 PBS and 3 ml of pH 8.8 sodium pyrophosphate buffer to bring the final pH of the solution to 8.8. The three electrodes were then submersed in the magnetically stirred solution, the working potential applied and 0.1 ml additions of 200 proof ethanol (17.1 M) were made in 20 s intervals. Initially, a working potential of +0.2 V was

used but failed to produce a good response even for the MWNT-based biosensor. Therefore, the working potential was increased to +0.3 V. The current generated by ethanol detection at the different biosensors is shown in Figure 4.7. As expected, the MWNT-based biosensor exhibited a much larger response to ethanol than the graphite- and CNF-based biosensors. It also showed a linear response within the tested concentration range and reached steady-state rapidly after each successive ethanol addition. Figure 4.8 shows a comparison of the responses of the graphite-, CNF- and MWNT-based biosensors to ethanol additions. The graphite- and CNF-based biosensors had responses that quickly decayed, indicating that the surface had become passivated.

The excellent sensitivity of the MWNT-based biosensor is a result of enhanced electron transfer kinetics between the nanotube-modified GC electrode and NADH. As previously discussed, the ability of MWNTs to promote electron transfer has been attributed to their electronic structure and electrical conductivity. Also, it has been proposed that electron transfer may be facilitated by the oxygen-containing functionalities on the surface of MWNTs which have been subjected to an oxidation treatment [40]. The relatively poor performance of the graphite-based biosensor is an expected result, since its structural anisotropy causes it to have a lower electrical conductivity than MWNTs. However, it is not entirely clear why the CNF-based biosensor exhibited performance more comparable to that of the graphite-based biosensor rather than the MWNT-based biosensor. While the manufacturer of the

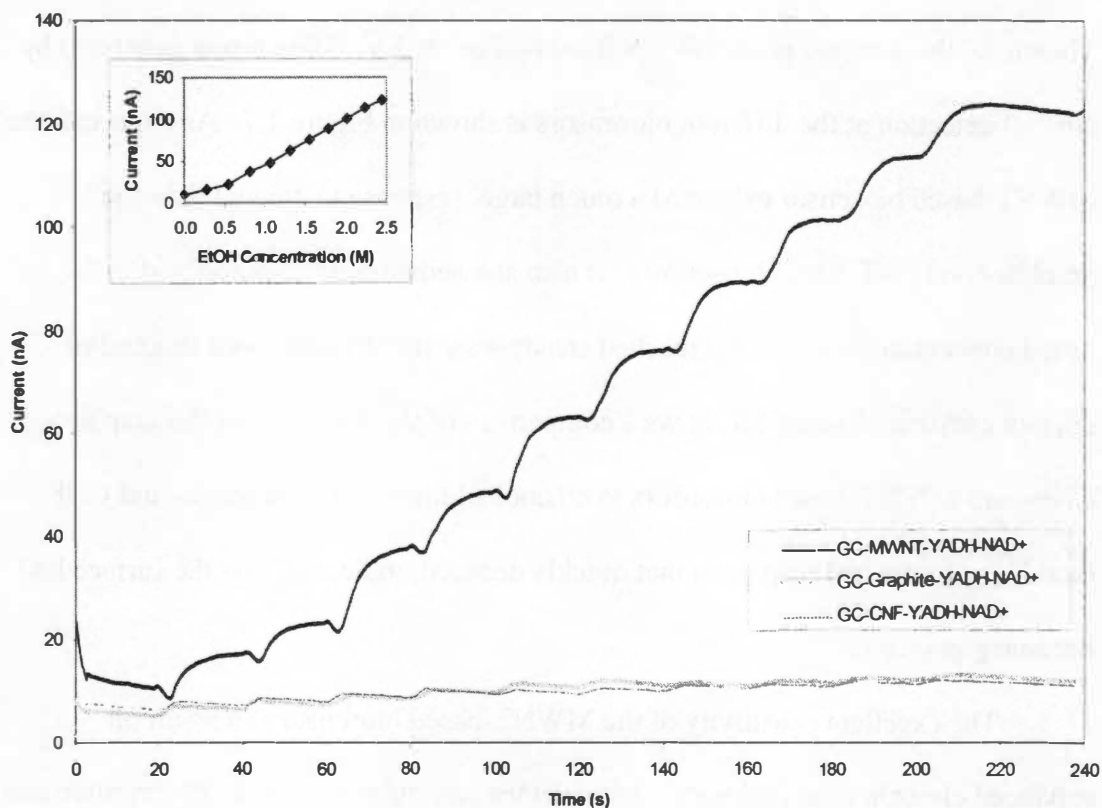


Figure 4.7: Amperometric detection of ethanol by graphite-, CNF- and MWNT-based biosensors.

The supporting electrolytes were pH 7.4 PBS and pH 8.8 sodium pyrophosphate; final pH of solution was 8.8. The solution was magnetically stirred at 400 rpm and the working potential was +0.3 V. The inset shows the current as a function of ethanol concentration for the MWNT-based biosensor.

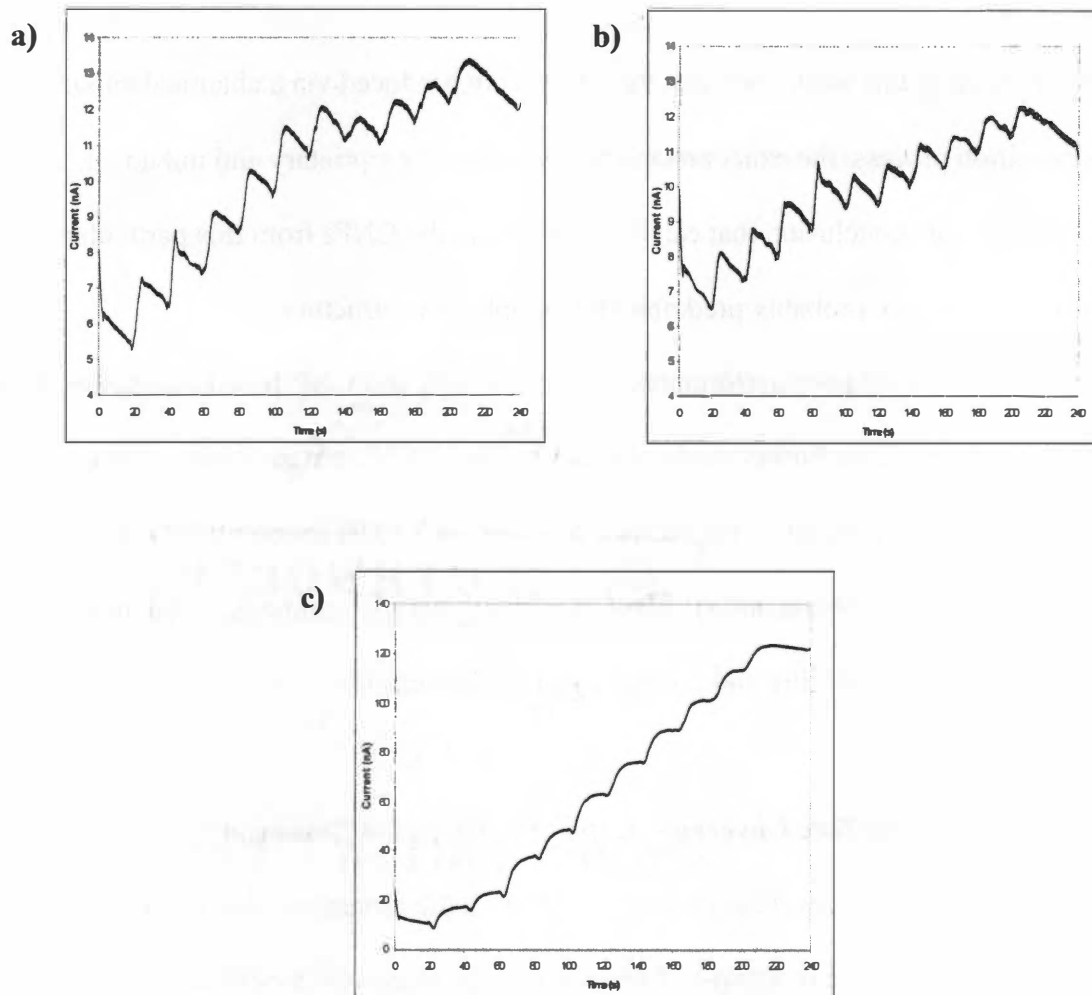


Figure 4.8: Individual responses of different biosensors to ethanol additions.

Responses of graphite (a)-, CNF (b)- and MWNT (c)-based biosensors to successive ethanol additions. Supporting electrolytes were pH 7.4 PBS and pH 8.8 sodium pyrophosphate; final pH of solution was 8.8. The solution was magnetically stirred at 400 rpm and the working potential was +0.3 V.

CNFs used in this work state that their fibers are produced via a chemical vapor deposition process, the exact process they employ is proprietary and unknown. As such, the only conclusion that can be made is that the CNFs from this particular manufacturer are probably predominately graphitic in structure.

Due to the poor performance of the graphite- and CNF-based biosensors, they were excluded from further study. However, the MWNT-based biosensor was studied more extensively. The surface coverage of YADH immobilized on the biosensor via adsorption and covalent attachment was determined as well as the enzyme kinetics, stability and reusability of the biosensor.

4.3 Enzyme Surface Coverage on the MWNT-based Biosensor

The surface coverage of active YADH on the biosensor was determined using a spectrophotometric technique. First, the GC electrode was modified by depositing MWNTs and YADH on its surface. The enzyme was either adsorbed to the surface of the modified electrode or covalently attached via EDAC-activated amidation. The coenzyme was not incorporated into the biosensor for this experiment. Instead, 1 ml of 5 mM NAD⁺ was placed in a quartz cuvette along with 1 ml of pH 8.8 sodium pyrophosphate buffer and 0.1 ml of ethanol. Next, the enzymatic reaction was initiated by submersing the biosensor in the cuvette solution and stirring. Absorbance measurements were made at 340 nm (the maximum absorbance wavelength of NADH) in 30 s intervals for a total of 5 min by briefly removing the biosensor from the cuvette. All absorbance values were recorded relative to the absorbance before

the reaction was initiated. The absorbance data were plotted against time and the slope of the line was used to calculate the units (U) of enzyme activity on the surface of the biosensor, where 1 U is defined as the amount of enzyme required to transform one micromole of ethanol per minute.

The activity observed for the biosensor with enzyme adsorbed on its surface was about 60 mU. This corresponds to a surface coverage of 1×10^{-12} mol of active enzyme, which accounts for almost 2% of the enzyme initially adsorbed on the surface. The biosensor with the covalently attached enzyme exhibited an activity of 20 mU which corresponds to a surface coverage of 3×10^{-13} mol of active enzyme. In this case, only 0.5% of the enzyme applied to the biosensor surface retained its activity, however, this is not an unexpected result since enzyme immobilization via covalent attachment typically has a more detrimental effect on activity than other immobilization techniques.

4.4 Enzyme Kinetics of the MWNT-based Biosensor

Determining the apparent enzyme kinetics of a biosensor is important since it allows one to identify the rate-determining step in analyte detection. For the MWNT-based biosensor, the apparent enzyme kinetics of adsorbed and covalently attached YADH were determined using the same amperometric detection technique that was described earlier. That is, the biosensor was submerged in a stirred solution of pH 7.4 PBS, a working potential of +0.3 V was applied and 0.1 ml ethanol additions were made every 20 s. The only difference is that ethanol additions were made over a 13

min period, whereas the previous experiments were conducted over a 4 min period.

Figure 4.9 shows the current as a function of time for the MWNT-based biosensor with adsorbed and covalently attached YADH and the current as a function of ethanol concentration is shown in Figure 4.10. Amperometric measurements were also performed for a MWNT-modified electrode with YADH and NAD^+ in free solution, The current response for these measurements is shown in Figure 4.11 and the current as a function of ethanol concentration is shown in Figure 4.12.

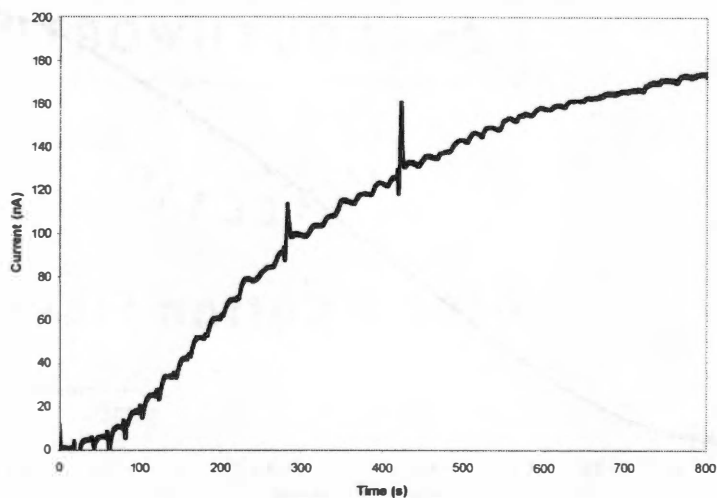
The curve in Figure 4.12 is described well by the Michaelis-Menten equation. A least squares fit of the Michaelis-Menten equation was performed on the data in the figure and an R^2 value of 0.9862 was obtained. The model parameters determined by the fit were: $i_m = 5400$ nA and $K_m^{app} = 0.99$ M. The curves in Figure 4.10 are not hyperbolic in shape, as would be expected if the enzyme exhibited Michaelis-Menten kinetics, but rather, they are more sigmoidal in shape. The Hill equation, shown in Equation 4.1, is a variation of the Michaelis-Menten equation that is capable of fitting sigmoidal data [40]. Typically, sigmoidal curves are indicative of allosteric

$$i = \frac{i_m [S]^n}{(K_m^{app})^n + [S]^n} \quad (4.1)$$

where, i = current
 i_m = maximum current
 $[S]$ = substrate concentration
 K_m^{app} = apparent Michaelis-Menten constant
 n = cooperativity coefficient

enzyme kinetics. Allosteric kinetics are often observed for enzymes which have multiple substrate binding sites and the binding of substrate to one site

a.)



b.)

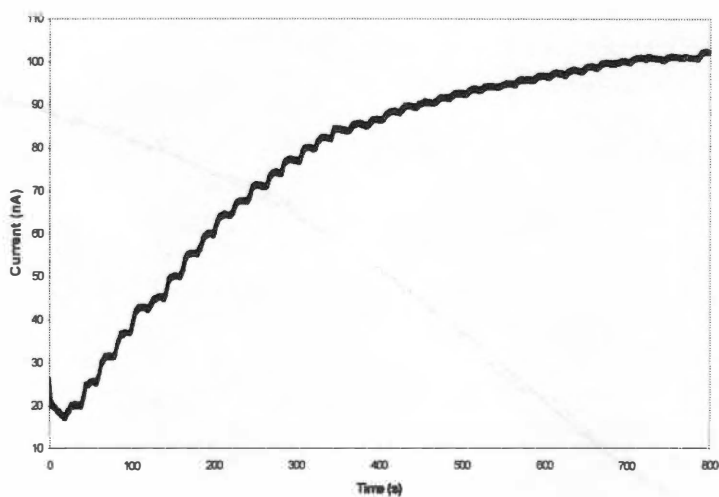


Figure 4.9: Amperometric detection of ethanol by two different MWNT-based biosensors.

Responses of adsorbed YADH (a) and covalently attached YADH (b) to successive ethanol additions. Supporting electrolyte was pH 7.4 PBS. The solution was magnetically stirred at 400 rpm and the working potential was +0.3 V.

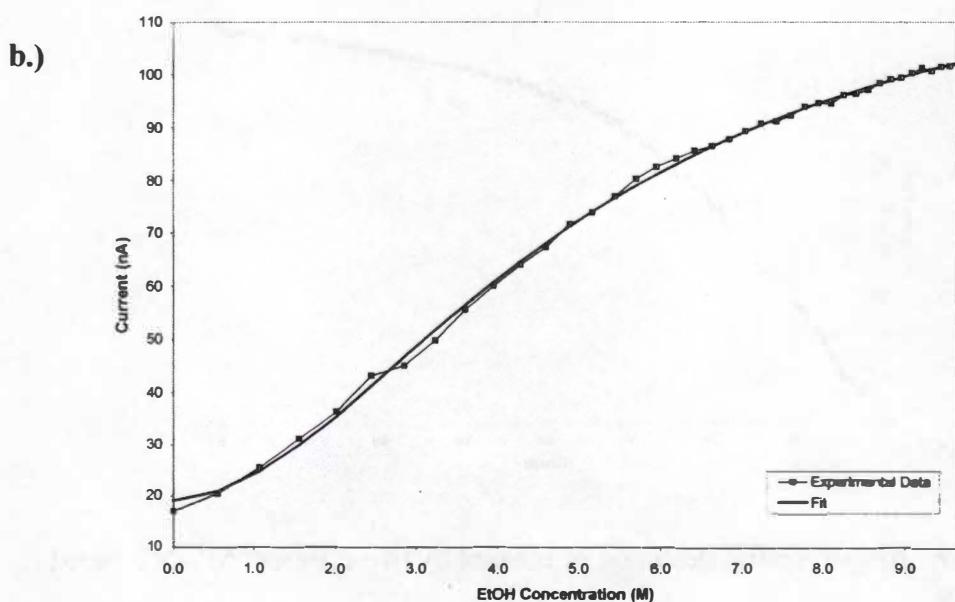
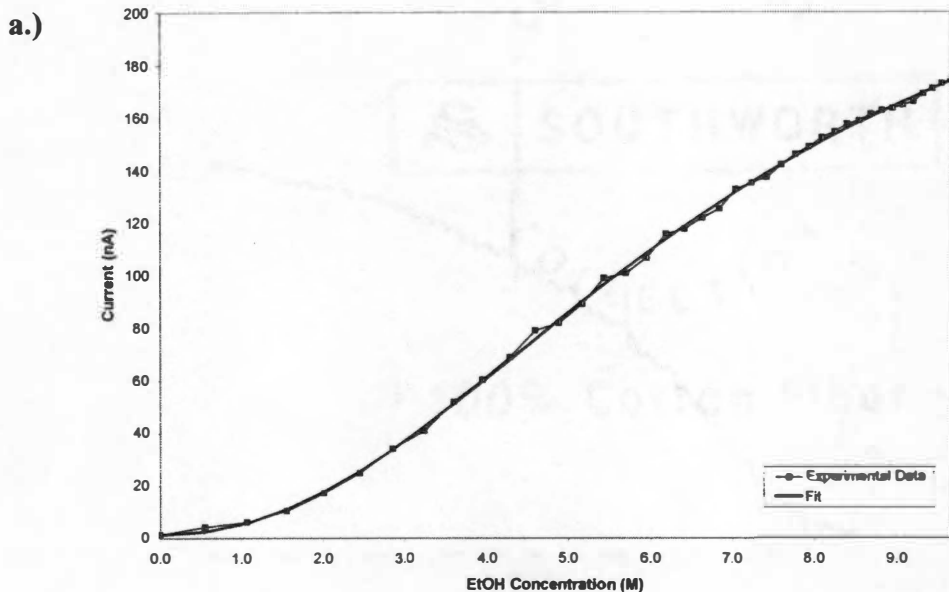


Figure 4.10: Current as a function of ethanol concentration for two different MWNT-based biosensors.

Experimental data and best fit curves for adsorbed YADH (a) and covalently attached YADH (b). Supporting electrolyte was pH 7.4 PBS. Solution was magnetically stirred at 400 rpm and the working potential was +0.3 V.

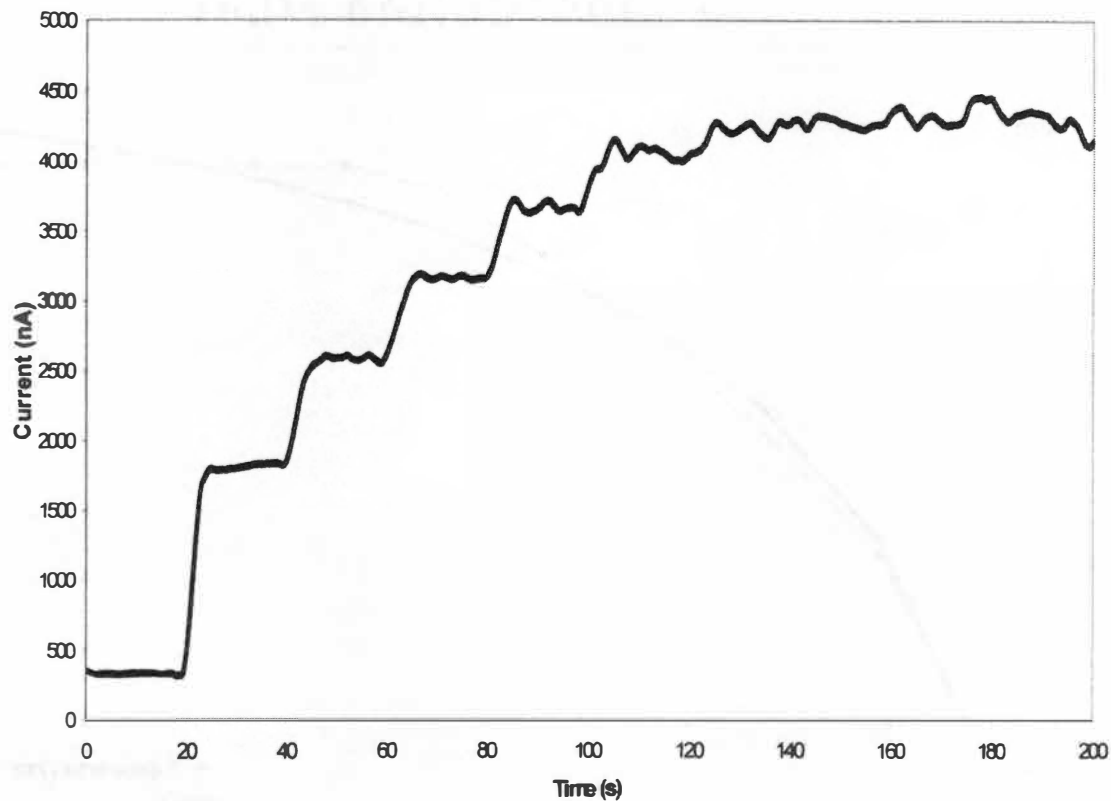


Figure 4.11: Amperometric detection of ethanol by the MWNT-modified electrode with YADH and NAD^+ in free solution.

Supporting electrolyte was pH 7.4 PBS. The solution was magnetically stirred at 400 rpm and the working potential was +0.3 V.

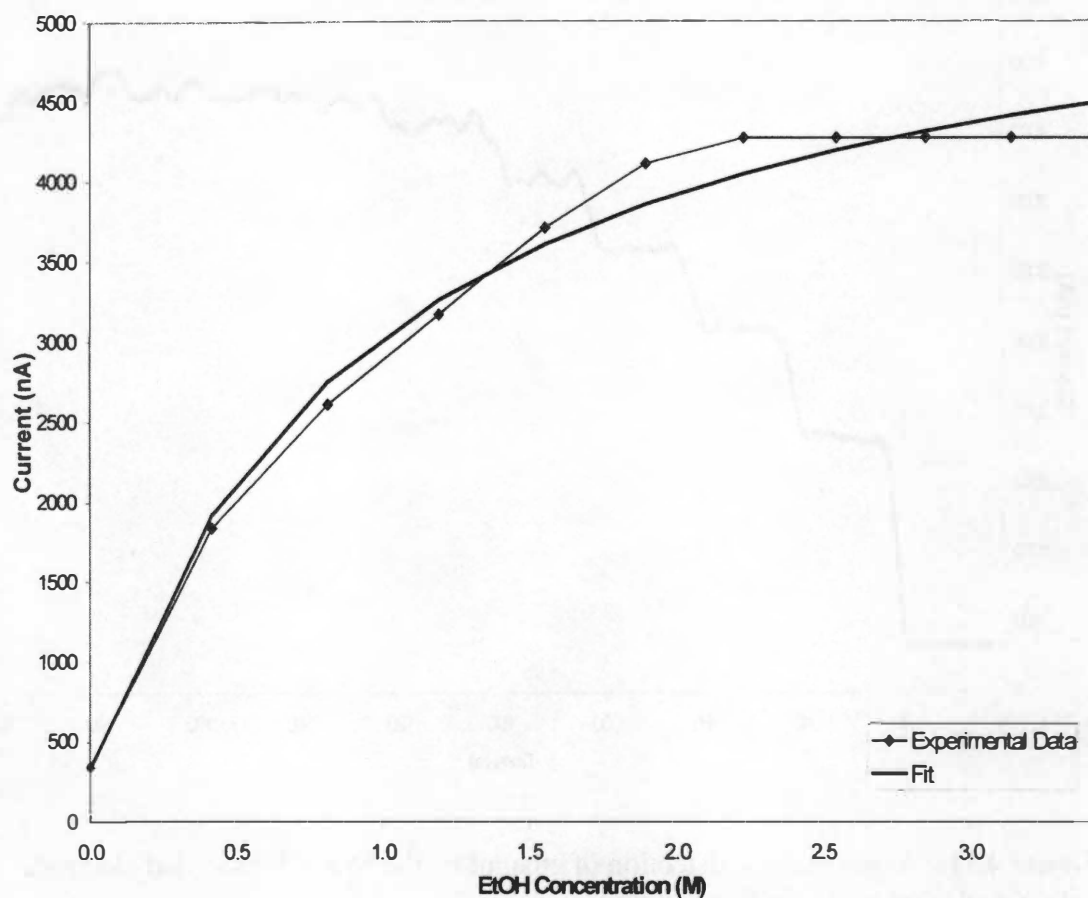


Figure 4.12: Current as a function of ethanol concentration for the MWNT-modified electrode with YADH and NAD^+ in free solution

Supporting electrolyte was pH 7.4 PBS. Solution was magnetically stirred at 400 rpm and the working potential was +0.3 V.

facilitates the binding of substrate to the remaining sites [41]. The degree of allostery is expressed as the cooperativity coefficient, n , in Equation 4.1. If $n = 1$, then Equation 4.1 reduces to the Michaelis-Menten equation, and if $n > 1$, then the equation will produce a sigmoidal curve indicative of positive cooperativity.

The Hill equation was fit to the experimental data in Figure 4.10 using the method of least squares and the resulting curves are also shown in the figure. For the MWNT-based biosensor with adsorbed YADH, the R^2 value for the fit was 0.9995 and the values of the adjustable parameters were as follows: $n = 2.2$, $i_m = 260$ nA and $K_m^{app} = 6.95$ M. For the biosensor with covalently attached YADH, the R^2 value was 0.9989 and the values of the adjustable parameters were: $n = 1.9$, $i_m = 110$ nA and $K_m^{app} = 5.10$ M. These results, as well as the results for the MWNT-modified electrode with YADH and NAD^+ in free solution, are summarized in Table 4.1.

It might be tempting to attribute the observed enzyme kinetics in Figure 4.10 to allosteric effects, however, YADH is known to follow true Michaelis-Menten kinetics (i.e. $n=1$) [42]. Most likely, the apparent allosteric kinetics and large values for K_m^{app} arise as a result of the rate-determining effect of substrate mass transport to the enzyme. This hypothesis is supported by the observed behavior of the MWNT-modified electrode in Figure 4.12. With the enzyme and coenzyme free in solution, the kinetics obeyed Michaelis-Menten kinetics and the K_m^{app} was much smaller than it was for either of the MWNT-based biosensors. For the MWNT-based biosensors, if we imagine the layer of MWNTs on the GC electrode as a tangled, three-dimensional

Table 4.1: Kinetic model parameters for MWNT-based biosensors and a MWNT-modified electrode

Parameter	MWNT-based Biosensors		MWNT-modified electrode
	Adsorbed YADH	Covalently attached YADH	
n	2.2	1.9	1.0
i_m	260 nA	110 nA	5400 nA
K_m^{app}	6.95 M	5.10 M	0.99 M

Parameters were determined by a least-squares fit of experimental kinetic data to the Hill equation (Equation 4.1) or the Michaelis-Menten equation.

matrix of nanotubes that has enzyme dispersed homogeneously within, then most likely, mass transport of substrate through the matrix would play a role in the determining the net reaction rate. Consequently, only the enzyme located near the surface of the biosensor will be exposed to the substrate at low bulk concentrations, and the resulting current will be small. As the bulk substrate concentration increases, the driving force for mass transport also increases and the substrate penetrates more deeply into the nanotube matrix. Since more enzyme is exposed to the substrate, more current is generated. Another possibility is that the mass transport limitations arise as a result of NAD^+ migration to the active site of the enzyme.

The most significant advantage associated with substrate mass transport being the rate-determining step in analyte detection is that the linear concentration range is extended relative to what it would be if the enzyme kinetics were rate-determining. For the MWNT-based biosensor with adsorbed enzyme, the largest linear concentration range lies between about 1.5 and 8.5 M ethanol (see Figure 4.10a). The biosensor response below 1.5 M ethanol is also relatively linear, but has a much smaller slope than the larger linear range. In other words, the biosensor displays poor sensitivity to ethanol at concentrations below 1.5 M. For the biosensor with covalently attached enzyme, the relatively linear concentration range lies between about 0.5 and 7.0 M ethanol (see Figure 4.10b). This biosensor appears to exhibit slightly better sensitivity than the previous one, however, its linear concentration range is not quite as large. One possible explanation for the different behaviors of the two biosensors may be that, for the biosensor with covalently attached enzyme, the

enzyme is concentrated more toward the surface of the biosensor rather than being homogeneously dispersed throughout the nanotube matrix. If this were the case, the biosensor would likely exhibit higher sensitivity and a decreased linear concentration range. However, there is no evidence to support this hypothesis, and as such, it is purely conjecture.

The large linear concentration ranges observed for both biosensors appear to be anomalous results when compared to the previously developed ethanol biosensors listed in Table 2.1. All of the previously developed biosensors had high sensitivities but limited linear concentration ranges. For example, the biosensor developed by Tobilina et al. (1999) had a linear concentration range of 45 μM – 4 mM. This biosensor was constructed by mixing chemically-modified carbon paste with YADH and NAD^+ in the dry state [16]. Castanon et al. (1997) also developed a biosensor using a chemically-modified carbon paste by adding an aqueous solution of the enzyme and coenzyme to the surface of the paste. The linear concentration range for this biosensor was 0.03 μM – 3 μM [19]. The biosensor developed by Wang and Musameh (2003) serves as a particularly good comparison since their working electrode was based on a MWNT/Teflon composite with YADH and NAD^+ adsorbed to its surface [20]. They observed Michaelis-Menten kinetics for the enzyme and a linear concentration range that extended to 1 mM ethanol. Their biosensor was more sensitive than those in this study, however, its linear concentration range was almost four orders-of-magnitude smaller.

4.5 Storage Stability of the MWNT-based Biosensor

The storage stabilities of the MWNT-based biosensors with adsorbed and covalently attached enzyme were determined by preparing the biosensors and allowing them to sit undisturbed at room temperature for a period of 5 days. The steady-state current was measured immediately after preparing the biosensors and again 5 days later by submerging them in a stirred solution of 2.4 M ethanol in pH 7.4 PBS and pH 8.8 sodium pyrophosphate buffer and applying a potential of +0.3 V. For both biosensors, there was a negligible current loss of less than 1%, between the initial and final measurements, indicating that both biosensors have excellent storage stability over a 5 day period at room temperature.

4.6 Reusability of the MWNT-based Biosensor

The reusability of each biosensor was determined by making repeated amperometric measurements in a stirred solution of 2.4 M ethanol in pH 7.4 PBS and pH 8.8 sodium pyrophosphate buffer at a potential of +0.3 V. The biosensor was removed from the solution and rinsed thoroughly with deionized water between measurements. This experiment was repeated in triplicate for both the adsorbed and covalently attached YADH biosensors. The results are shown in Figure 4.13 along with the standard deviations of the triplicate measurements. As can be seen in the figure, the reusabilities of both biosensors are statistically equivalent and the percentage of the original current remaining after ten measurements is approximately 70%.

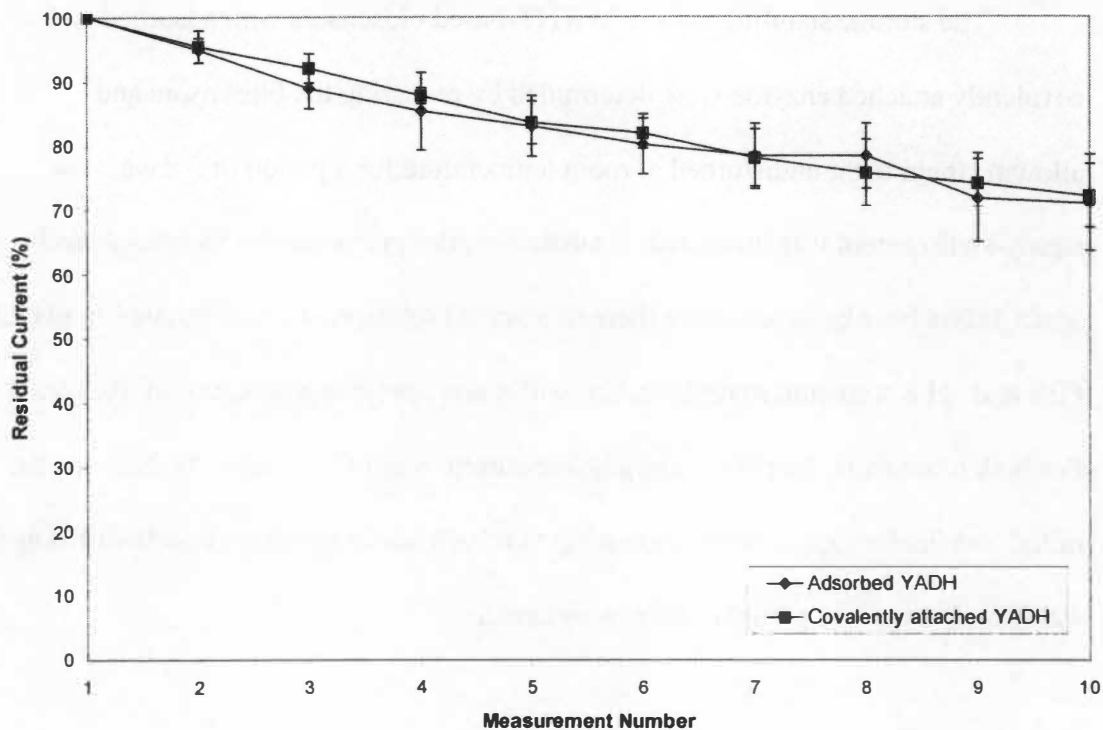


Figure 4.13: Reusability of two different MWNT-based biosensors.

Supporting electrolytes were pH 7.4 PBS and pH 8.8 sodium pyrophosphate; final pH of solution was 8.8. Ethanol concentration was 2.4 M. Solution was magnetically stirred at 400 rpm and the working potential was +0.3 V.

The fact that both biosensors displayed the same reusability suggests that some factor other than enzyme leakage or denaturation may be causing the steady decrease in biosensor response. If enzyme leakage were the problem, then the covalently attached biosensor should have showed a better reusability than the adsorbed one. The same argument can be made for the case where enzyme denaturation causes the response degradation. One explanation that could account for the results is NAD^+ leakage from the biosensor. However, this possibility was tested by reapplying NAD^+ to each biosensor immediately following the last measurement and then making an eleventh amperometric measurement. The resulting current was found to be the same as the previous measurement. Given this information, the most likely explanation for the biosensor response degradation is that the MWNT surface becomes passivated as the repeated measurements are conducted.

CHAPTER 5 CONCLUSION

The primary objective of this research was to develop a reagentless, amperometric ethanol biosensor based on YADH and NAD^+ immobilized on a MWNT-modified GC electrode. The performance of this biosensor was compared to that of graphite- and CNF-based biosensors as well as any previously developed amperometric ethanol biosensors found in the literature. In evaluating biosensor performance, several key characteristics were investigated including low-potential analyte detection, linear concentration range, stability and reusability.

The MWNT-based biosensor was found to have a much better overall performance than the graphite- and CNF-based biosensors. A relatively large response to ethanol at a working potential of +0.3 V (vs. Ag/AgCl) was observed for the MWNT-based biosensor. Also, both the MWNT-based biosensors with adsorbed and covalently attached YADH were found to exhibit excellent storage stability and their reusabilities were similar as well, with both losing approximately 30% of their response after 10 repeated amperometric measurements. Both biosensors had quite large linear concentration ranges of 1.5-8.5 M and 0.5-7.0 M ethanol, respectively. However, the sensitivities of these biosensors were not as high as expected. In fact, the performance of these biosensors was completely opposite to that of many previously developed ethanol biosensors which had high sensitivities but linear concentration ranges that extended into millimolar concentrations of ethanol.

There are a number of recommendations which can be made for future work on an amperometric ethanol biosensor. First, CNFs should be investigated more thoroughly as a working electrode material since the ones used in this study were from a particular supplier and the exact process employed for their production is unknown. The potential of using CNFs in electrochemical applications has already been shown, and their low-cost should be an impetus to employing them more often in amperometric biosensors. Future work might also focus on understanding why the performance of the biosensors in this study differed so strikingly from the previously developed ethanol biosensors. In order to address this issue, experiments should be performed that will definitively identify the rate-determining step in analyte detection. As mass transport is the suspected rate-determining step for the biosensor in this study, the focus should be on determining whether the mass transport limitations are due to the substrate or coenzyme. A couple of simple experiments could be performed to rule out mass transport limitations involving the coenzyme. First, the coenzyme could be included in free solution instead of on the surface of the biosensor when amperometric measurements were made. Also, the coenzyme could be mixed with the enzyme in aqueous solution prior to their incorporation in the biosensor. A final recommendation for future work would be to incorporate conductive polymers such as polyaniline into the MWNT-based biosensor. This has been done with some other amperometric biosensors and can serve to increase sensitivity and stability.

BIBLIOGRAPHY

Bibliography

1. Zhang S, Wright G, Yang Y (2000) Materials and techniques for electrochemical biosensor design and construction. *Biosens. Bioelectron.* **15**: 273-282.
2. Nylander C (1985) Chemical and biological sensors. *J. Phys. E: Sci. Instrum.* **18**: 736-750.
3. Nakamura H and Karube I (2003) Current research activity in biosensors. *Anal. Bioanal. Chem.* **377**: 446-468.
4. O'Connell PJ and Guilbalt GG (2001) Future trends in biosensor research. *Anal. Lett.* **34**(7): 1063-1078.
5. Nakamura R, Muguruma H, Karube I (1996) A novel method of immobilizing antibodies on a quartz crystal microbalance using plasma-polymerized films for immunosensors. *Anal. Chem.* **68**: 1695-1700.
6. Turner APF, Karube I, Wilson GS, eds (1987) *Biosensors: Fundamentals and Applications*. Oxford University Press, New York.
7. Kissinger PT and Heineman WH, eds (1996) *Laboratory Techniques in Electroanalytical Chemistry*. 2nd ed. Marcel Dekker, New York.
8. Suzuki S and Karube I (1981) Bioelectrochemical sensors based on immobilized enzymes, whole cells and proteins. *Appl. Biochem. Bioeng.* **3**: 145-174.
9. http://www.gamry.com/App_Notes/Potentiostat_Primer.htm
10. <http://www.iupac.org/goldbook/M03892.pdf>
11. Liu S-Q and Ju H-X (2002) Renewable reagentless hydrogen peroxide sensor based on direct electron transfer of horseradish peroxidase immobilized on colloidal gold-modified electrode. *Anal. Biochem.* **307**: 110-116.
12. Kong Y-T, Boopathi M, Shim Y-B (2003) Direct electrochemistry of horseradish peroxidase bonded on a conducting polymer-modified glassy carbon electrode. *Biosens. Bioelectron.* **19**: 227-232.
13. Chi EY, Krishnan S, Randolph TW, Carpenter JF (2003) Physical stability of proteins in aqueous solution: mechanism and driving forces in nonnative protein aggregation. *Pharm. Res.* **20**(9): 1325-1334.

14. Leskovac V, Trivić S, Peričin (2002) The three zinc-containing alcohol dehydrogenases from baker's yeast, *Saccharomyces cerevisiae*. *FEMS Yeast Research* 2: 481-494.
15. Yao Q, Yabuki S, Mizutani F (2000) Preparation of a carbon paste/alcohol dehydrogenase electrode using polyethylene glycol-modified enzyme and oil-soluble mediator. *Sens. Actuators, B.* 65(1-3): 147-149.
16. Tobalina F, Pariente F, Hernandez L, Abruna HD, Lorenzo E (1999) Integrated ethanol biosensors based on carbon paste electrodes modified with [Re(phen-dione)(CO)(3)Cl] and [Fe(phen-dione)(3)](PF6)(2). *Anal. Chim. Acta.* 395(1-2): 17-26.
17. Tobalina F, Pariente F, Hernandez L, Abruna HD, Lorenzo E (1998) Carbon felt composite electrodes and their use in electrochemical sensing: a biosensor based on alcohol dehydrogenase. *Anal. Chim. Acta.* 358(1): 15-25.
18. Mullor SG, SanchezCabezudo M, Ordieres AJM, Ruiz BL (1996) Alcohol biosensor based on alcohol dehydrogenase and Meldola Blue immobilized into a carbon paste electrode. *Talanta.* 43(5): 779-784.
19. Castanon MJL, Ordieres AJM, Blanco PT (1997) Amperometric detection of ethanol with poly-(o-phenylenediamine)-modified enzyme electrodes. *Biosens. Bioelectron.* 12(6): 511-520.
20. Wang J, Musameh M (2003) Carbon nanotube/teflon composite electrochemical sensors and biosensors. *Anal. Chem.* 75: 2075-2079.
21. Leca B and Marty J-L (1997) Reagentless ethanol biosensor based on a NAD-dependent dehydrogenase. *Biosens. Bioelectron.* 12(11): 1083-1088.
22. Ganzhorn AJ, Green DW, Hershey AD, Gould RM, Plapp BV (1987) Kinetic characterization of yeast alcohol dehydrogenases. Amino acid residue 294 and substrate specificity. *J. Biol. Chem.* 262: 3754-3761.
23. Hayes JE and Velick SF (1954) Yeast alcohol dehydrogenase: molecular weight, coenzyme binding and reaction equilibria. *J. Biol. Chem.* 207: 225-244.
24. Drakesmith FG and Gibson B (1988) A combined electrochemical process for the regeneration of coenzymes. *J. Chem. Soc., Chem. Commun.* 22: 1493-1494.
25. Long Y-T and Chen H-Y (1997) Electrochemical regeneration of coenzyme NADH on a histidine modified silver electrode. *J. Electroanal. Chem.* 440: 239-242.

26. Baik SH, Kang C, Jeon C, Yun SE (1999) Direct electrochemical regeneration of NADH from NAD⁺ using cholesterol-modified gold amalgam electrode. *Biotechnol. Tech.* **13**: 1-5.
27. Prieto-Simón B, Fàbregas E (2004) Comparative study of electron mediators used in the electrochemical oxidation of NADH. *Biosens. Bioelectron.* **19**: 1131-1138.
28. Wu K, Ji X, Fei J, Hu S (2004) The fabrication of a carbon nanotube film on a glassy carbon electrode and its application to determining thyroxine. *Nanotechnol.* **15**: 287-291.
29. Dai H (2002) Carbon nanotubes: synthesis, integration, and properties. *Acc. Chem. Res.* **35**(12): 1035-1044.
30. Merkulov VI, Lowndes DH, Wei YY, Eres G, Voelkl E (2000) Patterned growth of individual and multiple vertically aligned carbon nanofibers. *App. Phys. Lett.* **76**(24): 3555-3557.
31. McKnight TE, Melechko AV, Guillorn MA, Merkulov VI, Doktycz MJ, Culbertson CT, Jacobson SC, Lowndes DH, Simpson ML (2003) Effects of microfabrication processing on the electrochemistry of carbon nanofiber electrodes. *J. Phys. Chem. B* **107**: 10722-10728.
32. Xu J-Z, Zhu J-J, Wu Q, Hu Z, Chen H-Y (2003) An amperometric biosensor based on the coimmobilization of horseradish peroxidase and methylene blue on a carbon nanotubes modified electrode. *Electroanal.* **15**(3): 219-224.
33. Cai CX and Chen J (2004) Direct electrochemistry of horseradish peroxidase at a carbon nanotube electrode. *Acta Chim. Sinica* **62**(3): 335-340.
34. Wang SG, Zhang Q, Wang R, Yoon SF (2003) A novel multi-walled carbon nanotube-based biosensor for glucose detection. *Biochem. Biophys. Res. Commun.* **311**: 572-576.
35. Murphy MA, Wilcox GD, Dahm RH, Marken F (2003) Adsorption and redox processes at carbon nanofiber electrodes grown onto a ceramic fiber backbone. *Electrochem. Commun.* **5**: 51-55.
36. Marken F, Gerrard ML, Mellor IM, Mortimer RJ, Madden CE, Fletcher S, Holt K, Foord JS, Dahm RH, Page F (2001) Voltammetry at carbon nanofiber electrodes. *Electrochem. Commun.* **3**: 177-180.

37. Huang W, Taylor S, Fu K, Lin Y, Zhang D, Hanks TW, Rao AM, Sun Y-P (2002) Attaching proteins to carbon nanotubes via diimide-activated amidation. *Nano Lett.* 2(4): 311-314.
38. Hazani M, Naaman R, Hennrich F, Kappes MM (2003) Confocal fluorescence imaging of DNA-functionalized carbon nanotubes. *Nano Lett.* 3(2): 153-155.
39. Musameh M, Wang J, Merkoci A, Lin Y (2002) Low-potential stable NADH detection at carbon nanotube-modified glassy carbon electrodes. *Electrochem. Commun.* 4: 743-746.
40. http://www-biol.paisley.ac.uk/kinetics/Chapter_5/chapter5_6.html
41. Shuler ML and Kargi F (2002) *Bioprocess Engineering: Basic Concepts*. 2nd Ed. Prentice Hall, Upper Saddle River, New Jersey.
42. Chen D-H and Liao M-H (2002) Preparation and characterization of YADH-bound magnetic nanoparticles. *J. Mol. Catal. B: Enzym.* 16: 283-291.

VITA

Justin Holland was born in Murray, Kentucky on October 28, 1979. He graduated from Camden Central High School in May of 1997. In August of that year, he entered the University of Tennessee at Knoxville and obtained his Bachelor of Science degree in Chemical Engineering in May of 2002. He then began work on a Master of Science degree in Chemical Engineering at the University of Tennessee at Knoxville and in August of 2004, received the degree.

Faint, illegible text, possibly bleed-through from the reverse side of the page.

SOUTHWORTH

100% Cotton Fiber

1331 4702 16
12/28/04
HFB